Ion binding by humic and fulvic acids: A computational procedure based on functional site heterogeneity and the physical chemistry of polyelectrolyte solutions

J A Marinsky[1], M M Reddy[1], J Ephraim[2] and A Mathuthu[3]

[1] U S Geological Survey, Denver Federal Center, Lakewood, USA
[2] Linköping University, Department of Water in Environment and Society, Linköping, Sweden
[3] Department of Chemistry, State University of New York at Buffalo, Buffalo, New York, USA

April 1988

SKB - TR - 88-04

ION BINDING BY HUMIC AND FULVIC ACIDS: A COMPUTATIONAL PROCEDURE BASED ON FUNCTIONAL SITE HETEROGENEITY AND THE PHYSICAL CHEMISTRY OF POLYELECTROLYTE SOLUTIONS

J A Marinsky[1], M M Reddy[1], J Ephraim[2] and A Mathuthu[3]

1 U S Geological Survey, Denver Federal Center, Lakewood, USA

2 Linköping University, Department of Water in Environment and Society, Linköping, Sweden

3 Department of Chemistry, State University of New York at Buffalo, Buffalo, New York, USA

April 1987

ION BINDING BY HUMIC AND FULVIC ACIDS: A COMPUTATIONAL PROCEDURE BASED ON FUNCTIONAL SITE HETEROGENEITY AND THE PHYSICAL CHEMISTRY OF POLYELECTROLYTE SOLUTIONS

J.A. Marinsky, M.M. Reddy, J. Ephraim*, and A. Mathuthu**

U.S. Geological Survey, Denver Federal Center, Lakewood, CO 80225

* Linköping University, Department of Water in Environment and Society, Linköping, Sweden S-581 83

** Department of Chemistry, State University of New York at Buffalo, Buffalo, New York 14214

CONTENTS

ABSTRACT

Ion binding equilibria for humic and fulvic acids are examined from the point of view of functional site heterogeneity and the physical chemistry of polyelectrolyte solutions. A detailed explanation of the potentiometric properties of synthetic polyelectrolytes and ion-exchange gels is presented first to provide the basis for a parallel consideration of the potentiometric properties exhibited by humic and fulvic acids. The treatment is then extended to account for functional site heterogeneity. Sample results are presented for analysis of the ion-binding reactions of a standard soil fulvic acid (Armadale Horizons Bh) with this approach to test its capability for anticipation of metal ion removal from solution. The ultimate refined model is shown to be adaptable, after appropriate consideration of the heterogeneity and polyelectrolyte factors, to programming already available for the consideration of ion binding by inorganics in natural waters.

1 INTRODUCTION

Ionic interaction in natural waters is influenced by the presence of dissolved organic matter whose solution chemistry is not well understood. Rather than existing as a recognizable entity the humic and fulvic acids exist as a mixture of different functionalities in molecules which vary in size /1/. In humic and fulvic acids several different carboxylic acid moieties, whose acidities depend on their aromatic or aliphatic nature and their proximity to electron withdrawing functional groups, typically occur together with a small quantity of acidic alcohol /2/. In Armadale FA, for example, weakly acidic phenolic groups, and to a much smaller extent, amino groups, are in a position ortho to as much as 25 to 35% of the carboxylic acid moieties to provide bidentate chelating groups with strong metal-ion complexation capabilities /2/. The weakly acidic alcohol, ortho to another much less acidic hydroxyl or a carbonyl unit provides additional bidentate metal complexation pathways (e.g., catechol- and acetyl acetonate-like) /2/.

As a consequence of functional group heterogeneity inherent in natural organic material it is difficult to interpret ion-interactions in natural water systems containing high concentrations of humic and fulvic acids. In addition, the existence of a sequence of ionizable groups in one molecule endows polyelectrolyte properties to the organic assembly; the electric field at the surface of the molecule further complicates analysis of the properties of these systems. Prediction of ion-ion interaction in these systems has been uncertain while rationalization of observation has met with limited success.

In attempts that have been made to model proton binding by humic and fulvic substances, the need for separate consideration of the polyelectrolyte and heterogeneity factors was not appreciated. Indeed, in most of the models proposed, observed properties were interpreted using only one of these two factors. In the site-binding model /3-5/, one of the several most frequently employed, intrinsic acid dissociation constant values (pK) and abundances were assigned to the smallest number of monoprotic acids that reproduced the potentiometric data for a fixed, arbitrarily chosen, set of experimental conditions. However, because of neglect of the polyelectrolyte nature of humic and fulvic acids, electrolyte concentration effects could not be incorporated into data obtained at different salt concentration levels.

In other attempts to interpret the potentiometric behaviour of humic substances continuum models were examined /6-10/. In this

approach polyelectrolyte perturbations were ignored. The existence of a continuum of binding sites that is implied in these distribution models is believed by us to overestimate the complexity of the problem as well.

In the third kind of model generally employed all deviations encountered were attributed to the polyelectrolyte characteristics of the humic substances /11-19/. However, Posner /18/, as early as 1964, recognized that this kind of model could not account for the effect of ionic strength on the potentiometric properties. He correctly concluded that the observed behaviour was additionally complicated by the presence of different acidic functional groups in the humic substances molecule.

Marinsky and coworkers were the first to separate the functional group heterogeneity and polyelectrolyte effects /2/. They were able to assess accurately the contribution of polymeric properties to the potentiometric properties. With this capability, the heterogeneity factor became accessible, through use of a limited site model.

With the capability for quantifying the protonation properties of humic and fulvic acids available for the first time it has been possible to develop an approach which anticipates the interaction of metal ions with these natural organic acids. The basis of the approach to the computational scheme that is eventually presented in this manuscript is developed next in the text that follows.

2 THE TWO-PHASE MODEL

Our examination of the response of counter ion equilibria to simple neutral salt concentration levels in the presence of charged polymeric molecules has led to the development of a unified model which explains ion binding equilibria in polyelectrolyte and gel systems /20, 21/. This two-phase model leads to both a description of counterion distributions at equilibrium, and insight with respect to the conformation (rigid or flexible), permeability (to simple salt; hydrophilic or hydrophobic), and volume of the polymeric phase. What appears to be a homogeneous solution may be depicted as being composed of two separate phases.

2.1 DEVELOPMENT OF THE TWO-PHASE MODEL

The applicability of the two-phase model is first demonstrated for weakly acidic, cross-linked gels where the separate phases are easily recognizable. Insights gained from different graphical representations of the data are detailed in the presentation to demonstrate fully the utility of the two-phase model. A parallel treatment of linear polyelectrolyte analogs of the gels is then presented to show that, although no macroscopic second phase is present, the linear polyelectrolyte analogs behave exactly like the gels.

2.1.1 The Salt-Permeable Gel

The equilibrium distribution of diffusible components HX, MX, and H_2O in the crosslinked weakly acidic gel, (HA), simple salt (MX) system is determined by the fact that their free energies are the same in the separate phases defined by the gel and the aqueous medium. At equilibrium the chemical potential, μ, of each diffusable component is thus identical in both phases as shown:

$$\mu_{HX} = \overset{o}{\mu}_{HX} + RT \ln a_{HX} = \bar{\mu}_{HX} = \bar{\overset{o}{\mu}}_{HX} + RT \ln \bar{a}_{HX} \quad (1)$$

$$\mu_{MX} = \overset{o}{\mu}_{MX} + RT \ln a_{MX} = \bar{\mu}_{MX} = \bar{\overset{o}{\mu}}_{MX} + RT \ln \bar{a}_{MX}$$

$$\mu_{H_2O} = \overset{o}{\mu}_{H_2O} + RT \ln a_{H_2O} = \bar{\mu}_{H_2O} = \bar{\overset{o}{\mu}}_{H_2O} + RT \ln \bar{a}_{H_2O}$$

In these equations the bar above a symbol identifies its association with the gel phase, "a" refers to activity and R and T have their usual meaning. Choosing the same standard state for each component in both phases leads to the cancellation of μ^o by $\bar{\mu}^o$ in equation (1) so that the activity ratio of the counterions in the two phases can eventually be equated as shown:

$$pH - pM = p\bar{H} - p\bar{M} \quad (2)$$

where the notation "p" always has its usual meaning, the negative logarithm (e.g., $pM = -\log a_M$).

In the examination of potentiometric data obtained for crosslinked, weakly acidic gels, it is convenient to plot the apparent pK, $pK^{app}_{(HA)_\nu}$, evaluated with the Henderson-Hasselbalch equation /22/ given below, versus α, the degree of dissociation

$$pH - \log \frac{\alpha}{1-\alpha} = pK^{app}_{(HA)_\nu} \quad (3)$$

where the subscript ν refers to the number of times the acidic functional unit is repeated in the molecule and K is defined as the dissociation constant. Such treatment of the potentiometric data results in the automatic inclusion of a Donnan /23/ term ($pM-p\bar{M}$) in the computed value of the apparent pK as shown:

$$pH - \log \frac{\alpha}{1-\alpha} = p\bar{H} - \log \frac{\alpha}{1-\alpha} - p\bar{M} + pM \quad (3b)$$

so that

$$pK^{app}_{(HA)_\nu} = p\bar{K}^{app}_{(HA)_\nu} + (pM-p\bar{M}) \quad (3c)$$

A consequence of this is that the measured pK, $pK^{app}_{(HA)_\nu}$, is always a sensitive function of the ionic strength of the system under investigation, plots of $pK^{app}_{(HA)_\nu}$ versus α tending to separate at different ionic strengths as the titration proceeds (Figure 1). One can expect to find that as α increases the curves will tend to parallel each other, with their vertical separation a function of the different salt concentrations employed in the potentiometric titrations. These predicted properties of the curves are expected

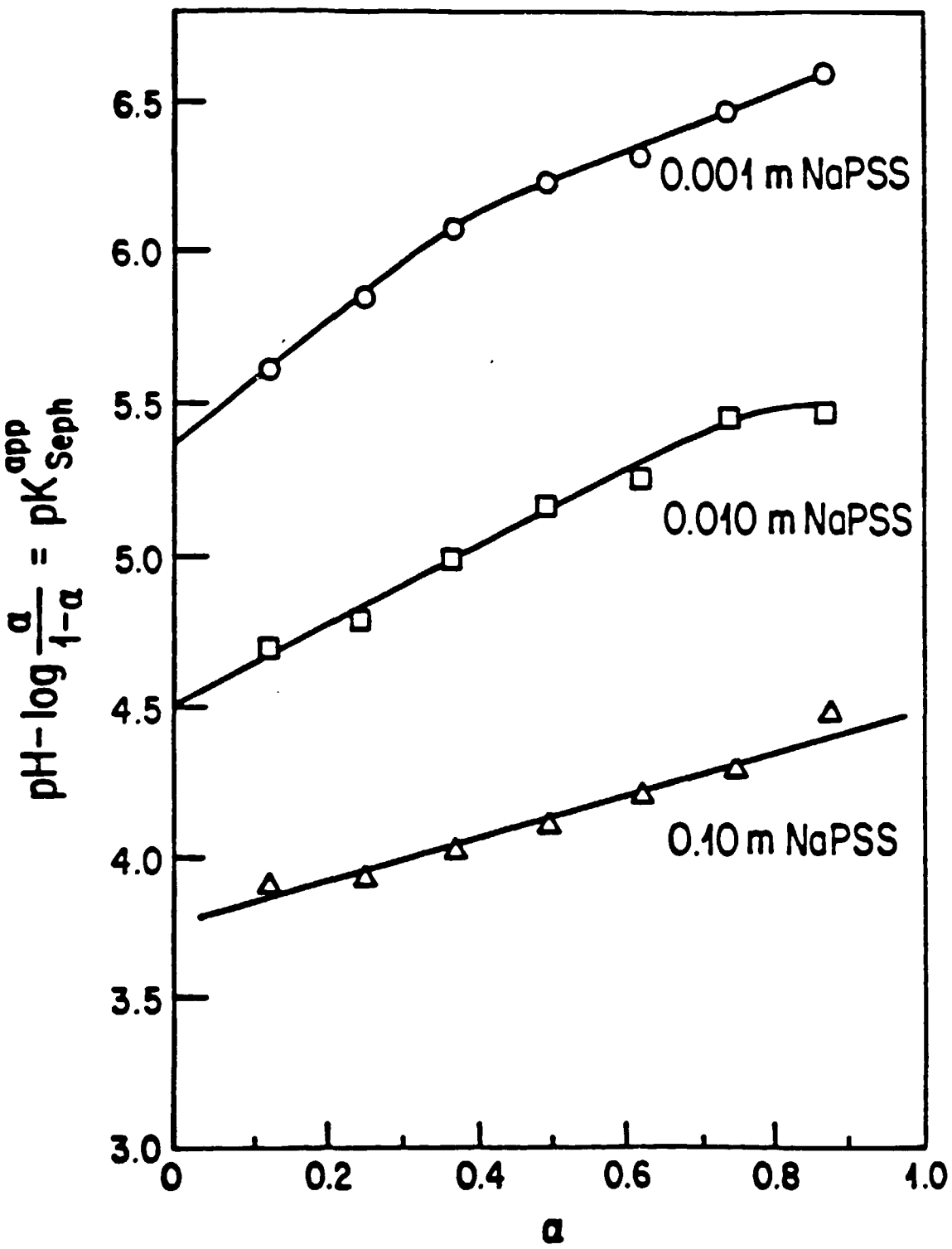

Figure 1. Potentiometric properties of the flexible Sepnadex CM 50-120 gel measured at three different sodium polystyrene-sulfonate concentration levels (Donnan potential term neglected).

to be most closely approximated when (1) the imbibed salt concentration level, $\bar{m}_s$, (where the subscript s refers to MX, the particular salt employed) is much less than the counterion concentration, $\bar{m}_M(\alpha\nu/V_p)$, of the gel and (2) the volume, V_p, of the gel is essentially independent of α because of its rigidity. When these conditions are met, $\bar{m}_M$ is a unique function of α that remains unaffected by changes in m_s. The vertical displacement of the curves thus equals $\Delta(pm_s)$ in value. In flexible gels the separation eventually reached in the curves at low salt concentration levels will always be smaller than $\Delta(pm_s)$.

Confirmation of the physical chemical description of the weakly acidic gel-salt system that is presented above has been provided by resolving the potentiometric properties of the gel itself. When this is done the intrinsic pK deducible from studying the neutralization at the site of the reaction is found to be identical to the literature-based pK value of the molecule most nearly resembling the repeating functional unit of the gel /24/. For example, we have shown that the $pK^{int}_{(HA)}$ value of 4.8±0.05 that is resolved in this way for a crosslinked polymethacrylic acid gel is identical with the pK value of 4.83 that has been reported for isobutyric acid /25/ which closely resembles the repeating functional unit of the gel.

To effect such resolution of the potentiometric data the Donnan potential term, the ratio of metal ion activities in the two phases ($pM-p\bar{M}$), had to be evaluated to obtain the value of the hydrogen ion activity within the gel ($p\bar{H}$) as a function of the degree of ionization /24/. For this purpose the water content of the gel, measured as a function of α in separate experiments at each ionic strength, was divided into $\alpha\nu$, the experimentally measured amount of dissociated acid ($bV_b + hV_s$); b and V_b represent the concentration and volume of standard base added and h and V_s refer to the hydrogen ion concentration and the volume of the solution after each addition of base. This quantity, equatable to the total counter ion content of the gel phase ($\Sigma M^+ + \Sigma H^+$) because of electroneutrality requirements in the gel phase, yielded an accurate estimate of $\bar{m}_M$ when divided by V_p because $\Sigma M^+ >>> H^+$ and the quantity of H^+ could be neglected without introduction of noticeable error.

By this approach $p\bar{m}_M$, and not $p\bar{M}$, was available for use in equation 2. As a consequence the value of $p\bar{m}_M$ resolved was used in place of $p\bar{H}$ in the Henderson-Hasselbalch equation for resolution of $p\bar{K}^{app}_{(HA)_\nu}$. This substitution of concentrations for activities was permissible because the nonideality of Na^+ and H^+ (Na^+ salts were used to define the ionic strength of the systems) in gels has been shown to be nearly the same /26/.

Plots of $p\bar{K}^{app}_{(HA)_\nu}$ versus α based on $p\bar{m}_H$ estimates made as described above, (Figures 2 and 3 for the flexible (Sephadex CM-50) and inflexible (Sephadex CM-25) gels, respectively), show that in the flexible gel $p\bar{K}^{app}_{(HA)_\nu}$ increases with α; the rate of increase of $p\bar{K}^{app}_{(HA)_\nu}$ with α is greater the lower the concentration of the

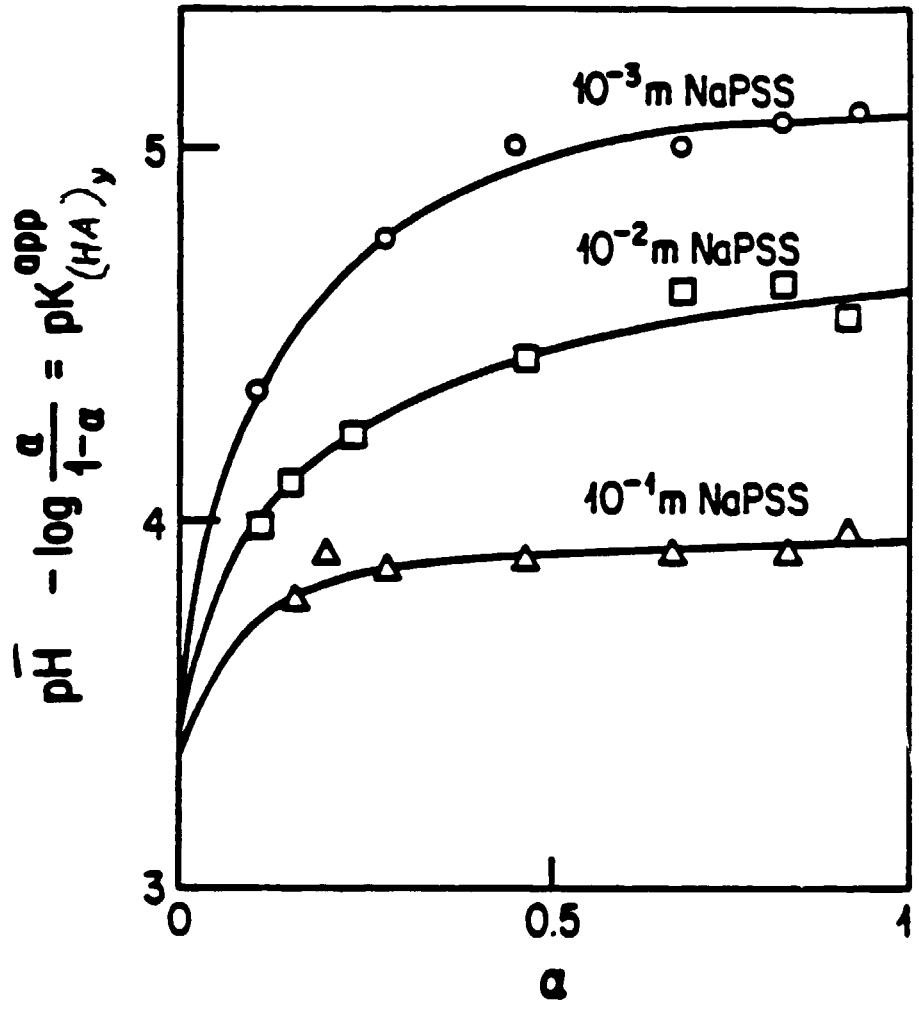

Figure 2. Potentiometric data of Figure 1 analyzed with inclusion of Donnan potential term.

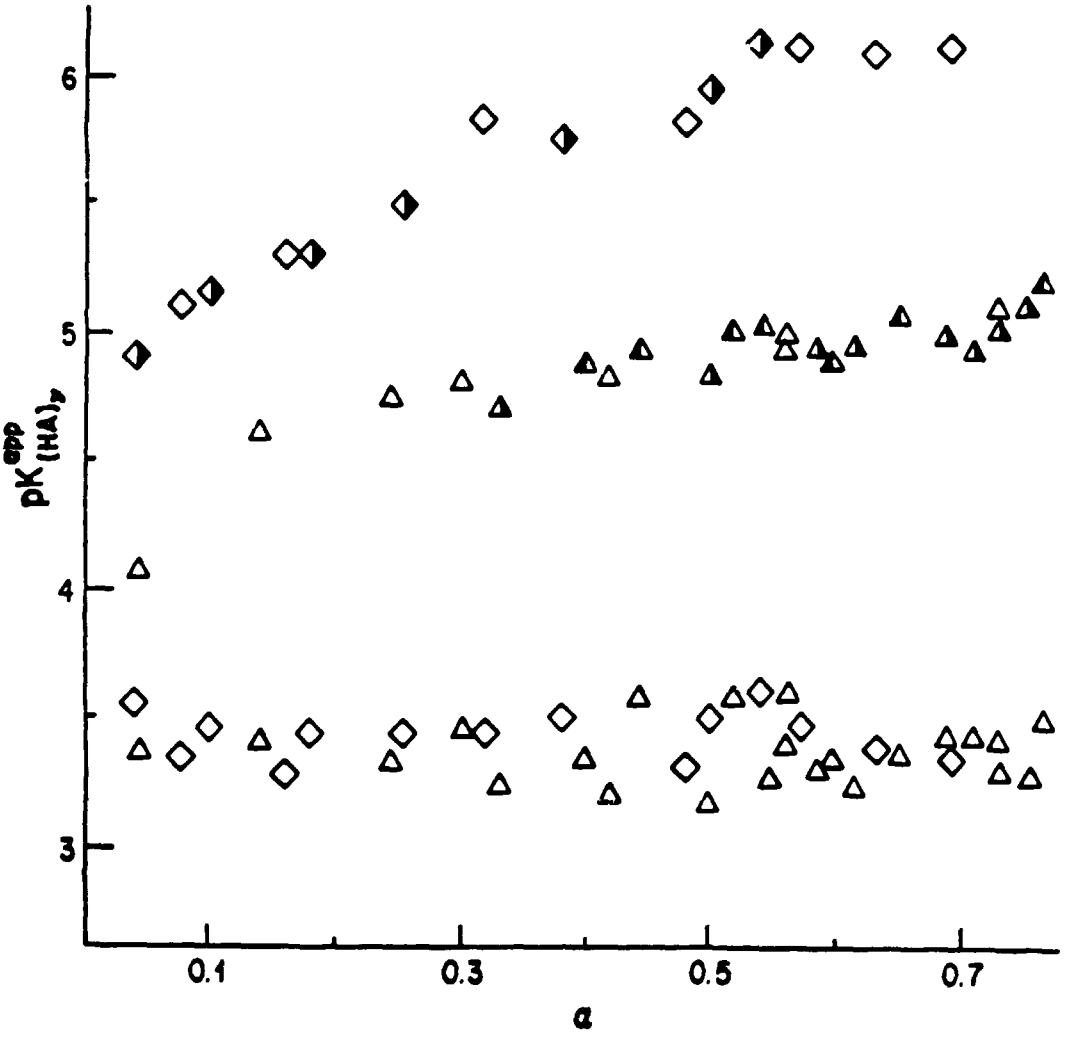

Figure 3. Potentiometric properties of the rigid Sephadex CM-25 gel measured in 0.0010 and 0.010 m sodium perchlorate; upper curves, Donnan potential term neglected; lower curve, Donnan potential term included.

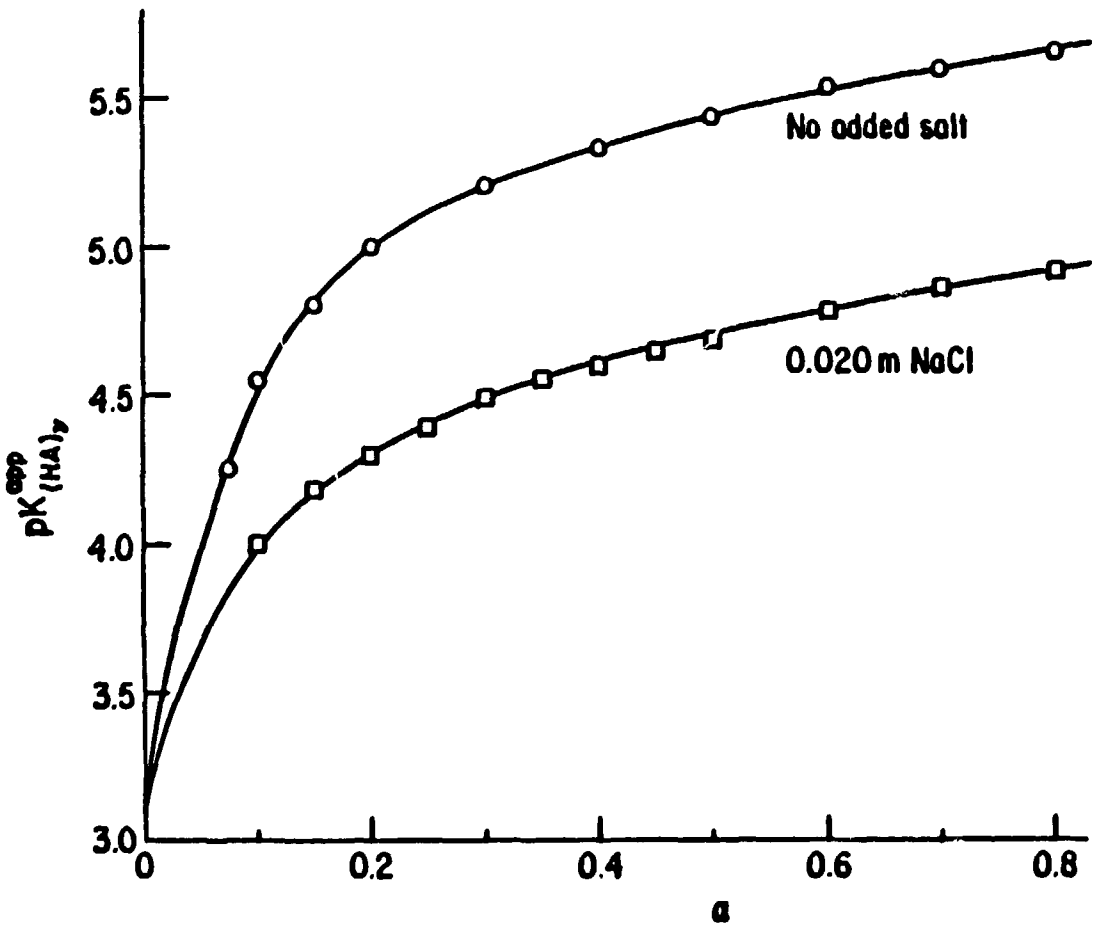

Figure 4. Dependence of potentiometric properties of carboxymethyldextran, the linear polyelectrolyte analogue of Sephadex, on salt medium concentration.

ionic medium. The $p\bar{K}^{app}_{(HA)_\nu}$ of the inflexible gel is unaffected by change in α.

Plots of $p\bar{K}^{app}_{(HA)_\nu}$ versus α presented in Figure 4 for carboxymethyldextran, the linear analog of the Sephadex gels /27/, show that the potentiometric behaviour of the flexible gel and its linear analog is comparable. As α decreases the curves in Figures 2 and 4 converge to the same common point yielding a $pK^{int}_{(HA)_\nu}$ value of 3.3±0.05 for the functional unit repeated throughout the full length of the polymer. This pK value is in good agreement with the pK value of 3.3 reported in the literature for methoxycarboxylic acid /25/, a molecule closely resembling the acidic site repeated throughout the carboxymethyldextran molecule and its cross-linked gel (Sephadex) analog.

For the inflexible Sephadex CM-25 (Figure 3) the $p\bar{K}^{app}_{(HA)_\nu}$ value of 3.3±0.08 resolved at different salt concentration levels is, as we have seen, independent of α and corresponds to the intrinsic pK, $p\bar{K}^{int}_{(HA)_\nu}$, evaluated by extrapolation of the curves in Figures 2 and 4. From this we have inferred that for a rigid gel equation 3c can be rewritten as follows:

$$p\bar{K}^{app}_{(HA)_\nu} = p\bar{K}^{int}_{(HA)_\nu} + (pM-p\bar{M}) \qquad (3d)$$

This important conclusion has been anticipitated for linear polyelectrolytes in the following Gedanken experiment as well. Using the cell model of solutions /28/ to describe the polyelectrolyte each cell is divided into microregions. The centrally located macroin of the cell is then presumed to establish an electrostatic potential which governs the distribution of counterions in these microregions. Prigogine et al. /29/ have shown that in the absence of salt, single ion potentials may be attributed to microscopic regions as long as they are small enough to be regarded as volume differentials yet large enough to contain a sufficiently large number of ions so the relative fluctuation in concentration is negligibly small. On this basis the equilibrium condition for $\bar{\mu}_i$, the electrochemical potential of the counter ion in any microregion of the cell, is that it be independent of its position in the cell and that it have the same value in the macroregions of the equilibrated system. In the presence of salt the electrochemical potential in the equilibrated system of both counter and coion may be considered to be independent of their position in the cell as well. With this condition we find that at equilibrium

$$pH-pM = p\vec{H}-p\vec{M} \qquad (2a)$$

where the arrow above H and M is used to identify the polymer domain. This result shows that the apparent pK measured for a weakly acidic polyelectrolyte is indeed expressed by equation 3d.

Thus, linear polyelectrolytes, when dissolved in solution, may be considered to be present in the solution as a separate phase just like their gel analogs. From a comparison of Figure 2 with Figure 4 we can also deduce that the gel phase of the flexible Sephadex CM-50 itself has such a high water content that the gel can be considered a two phase system (the gel water and the organic matrix) like its linear polyelectrolyte analog. The fact that the effect of ionic strength on the two sets of curves is so similar in the two figures leads to this conclusion.

Experimental documentation of the above observation that linear polyelectrolytes may be treated as a separate phase in solution is presented in a later section of this manuscript.

2.1.2 The Salt-Impermeable Gel

One can expect Poisson-Boltzmann statistics, used as shown in equations 4a and 4b given below, to express accurately the effective concentration of counterions in the domain of a salt-impermeable gel. By salt-impermeable gel we mean a gel which excludes ions of the same charge as the gel polyion from its boundaries. In equations 4a and 4b the arrow placed above the letter representation of H^+ and M^+ identifies the effective concentration of

$$(\vec{M}^+) = (M^+) \exp(-\varepsilon\psi(a)/kt) \tag{4a}$$

$$(\vec{H}^+) = (H^+) \exp(-\varepsilon\psi(a)/kt) \tag{4b}$$

these counterions inside the negatively charged gel relative to the effective average macroscopic concentrations measured potentiometrically, ε represents the unit charge of the ion, $\psi(a)$ corresponds to the potential due to the charge of the gel molecule, k is Boltzmann's constant and T is the absolute temperature of the system. At equilibrium the ratio of the activities of H^+ and M^+ in the solution is equal to their ratio in the gel domain.

$$\frac{(\vec{M}^+)}{(\vec{H}^+)} = \frac{(M^+)\exp(-\varepsilon\psi(a)/kt)}{(H^+)\exp(-\varepsilon\psi(a)/kt} = \frac{(M^+)}{(H^+)} \tag{5}$$

and equation 2a applies as before

$$\vec{pH}-\vec{pM} = pH-pM \tag{2a}$$

Once again the curves are separated at different ionic strengths in plots of $pK^{app}_{(HA)_\nu}$ versus α. In this instance, because there can be no imbibement of salt to change the metal ion concentration within the gel phase, the separation of the curves can be less than $\Delta(pm_s)$ only if (1) the gel is flexible and/or (2) the concentration of salt (m_{MX}) approaches the value of $\bar{m}_M$.

2.2 IMPLICATION OF THE TWO-PHASE MODEL

If the concentration of metal ion in the salt-permeable gel phase is much greater than in the solution phase the incursion of the gel by salt is negligible. If the gel is rigid as well the metal ion concentration within the gel is a uniquely defined quantity at each α value encountered no matter what the neutral salt (MX) concentration level. However, as the extent of polymer ionization approaches zero the accompanying reduction in the gel phase metal ion concentration approaches zero as well and some dependence of $\bar{m}_M$ on ionic strength eventually manifests itself. Over the α range where uniqueness of $\bar{m}_M$ prevails the $\bar{m}_H$ must also be uniquely defined at each α value. The free energy of dissociation of the acidic unit of the polymer in the reproduced environment insures this result. As a consequence, $p\bar{H}-p\bar{M}$ is independent of the external neutral salt concentration level (m_{MX}) and plots of $pK^{app}_{(HA)_\nu}$ versus (pH+pX) will yield a single unique curve that is unaffected by ionic strength /20,21/.

Such a plot of potentiometric data obtained with the rigid Sephadex CM-25 at several different concentration levels of $NaClO_4$ (0.10 to 0.0010 m) uniquely resolves the top curve (A) presented in Figure 5 to illustrate this. The two lower curves (B) of Figure 5 show that with the highly flexible CM-50 Sephadex gel the uniqueness of the plot is lost, the data obtained at each ionic strength yielding curves that eventually separate as the neutralization proceeds.

In a rigid, salt-impermeable gel the value of the gel phase metal ion concentration is uniquely defined at each polyion dissociation value as it is in the rigid salt-permeable gel. This in turn uniquely defines the gel phase hydrogen ion concentration, as before, since the free energy of dissociation of the functional units that constitute the rigid gel matrix cannot be a variable function of α in the reproducible environment at the molecular surface. As a consequence, the uniquely defined ratio of $(\vec{M}^+)/(\vec{H}^+)$ must also be mimicked in the aqueous solution with the salt-impermeable membrane as long as $(\vec{M}^+)$ is equal to or greater than the solution phase metal activity. When the gel phase metal concentration becomes equal to or smaller than the solution phase metal concentrations as α approaches zero the $(\vec{M}^+)/(\vec{H}^+)$ ratio can no longer control the $(M^+)/(H^+)$ ratio in solution. In this situation the charge on the surface of the molecule has to be close to zero and $(\vec{H}^+)$ approaches (H^+) in value. Because no salt can invade the gel, plots of $pK^{app}_{(HA)_\nu}$ versus pH alone are expected to be unaffected by the concentration level of the salt as long as $m_{MX} < \vec{m}_M$ (see for example Paterson and Rahman /30/.

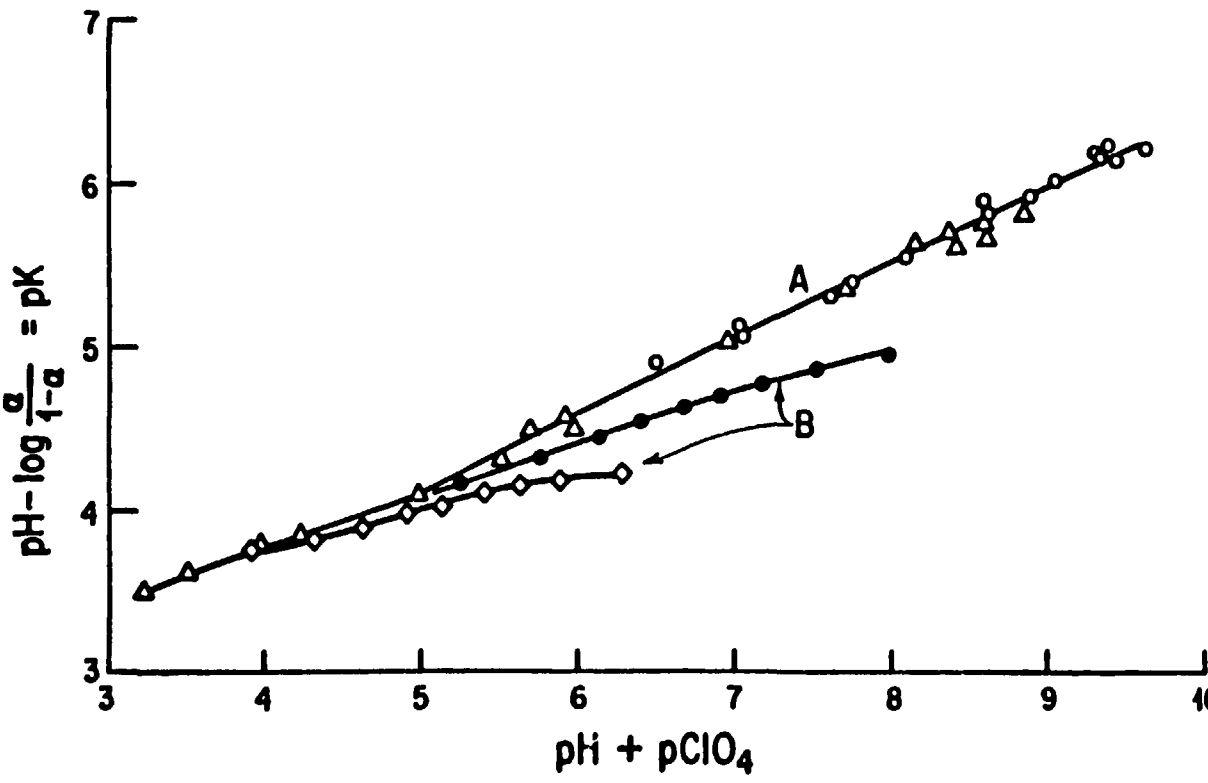

Figure 5. Behaviour at different $NaClO_4$ concentration levels of the $pK^{app}_{(HA)_v}$ parameter in a rigid (Sephadex CM-25) and flexible (Sephadex CM-50) gel framework when plotted vs ($pH+pClO_4$).

3 DOCUMENTATION OF THE APPLICABILITY OF THE TWO-PHASE MODEL TO POLYELECTROLYTE-SIMPLE NEUTRAL SALT SYSTEMS

Potentiometric data obtained with weakly acidic polyelectrolytes in solutions at different simple salt concentration levels yield apparent pK values that are either uniquely a function of (pH+pX) or pH alone, just like their gel analogs, supporting their description in aqueous media as a separate phase. This result is summarized briefly in Figures 6-11 /31-33/. In these figures $pK^{app}_{(HA)_\nu}$ is plotted versus (pH+pX) for the polyelectrolytes, poly(acrylic acid), poly(methacrylic acid) /31/, poly(D, L-glutamic acid), and poly(L-glutamic acid) /32/; for polyethyleneimine and poly(vinylamine) /33/, the apparent pK is plotted versus pH alone. Anion activity coefficients employed to evaluate the anion activity for use in the ordinate term were obtained from the single ion activity coefficient values based upon computation due to Kielland /34/ up to an ionic strength of 0.10, the upper range of their projected validity. Above this ionic strength the mean molal activity coefficient published for the uni-univalent salt was employed.

A single unique curve is obtained for poly(acrylic acid) (Figure 6) and poly(D,L-glutamic acid) (Figure 8) to show that these linear polyelectrolytes are rigid and permeable to salt. The divergence in $pK^{app}_{(HA)_\alpha}$ from the otherwise uniquely resolved curve in Figure 9 arises from the discontinuity attributable to conformational change in the poly(methacrylic acid) molecule from a compact to random coil configuration. This molecule is thus rigid and permeable to salt in both forms. With the poly(L-glutamic acid) molecules there is, using data due to Olander and Holtzer /32/, in Figure 9 a unique description of $pK^{app}_{(HA)_\nu}$, as a function of (pH+pX) only in the helix region. There is a divergence of curves after passing the discontinuities due to transition from the α-helix to its single strand conformation. From this result we can conclude that the α helix configuration is inflexible and permeable to salt; the single-stranded molecule is, on the other hand, apparently quite flexible and hydrophilic.

Finally, the resolution of a single curve when $pK^{app}_{(HA)_\nu}$, is plotted versus pH alone for polyethylenimine and poly(vinylamine) in Figures 10 and 11 assigns rigidity and salt impermeability to these hydrophobic polyelectrolytes.

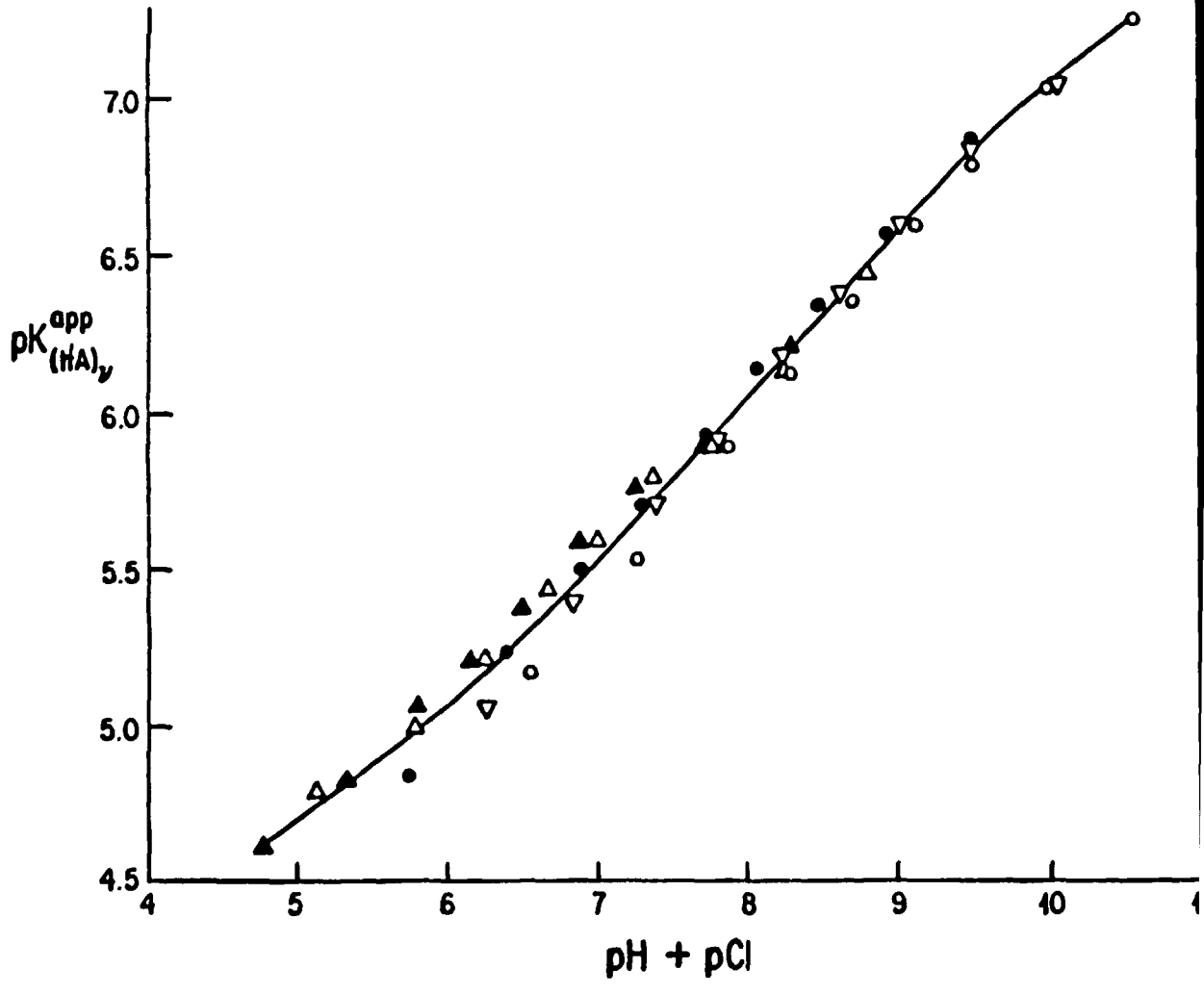

Figure 6. A plot of apparent pK versus (pH+pCl) values for poly (acrylic acid) using potentiometric data compiled at five different sodium chloride concentrations.

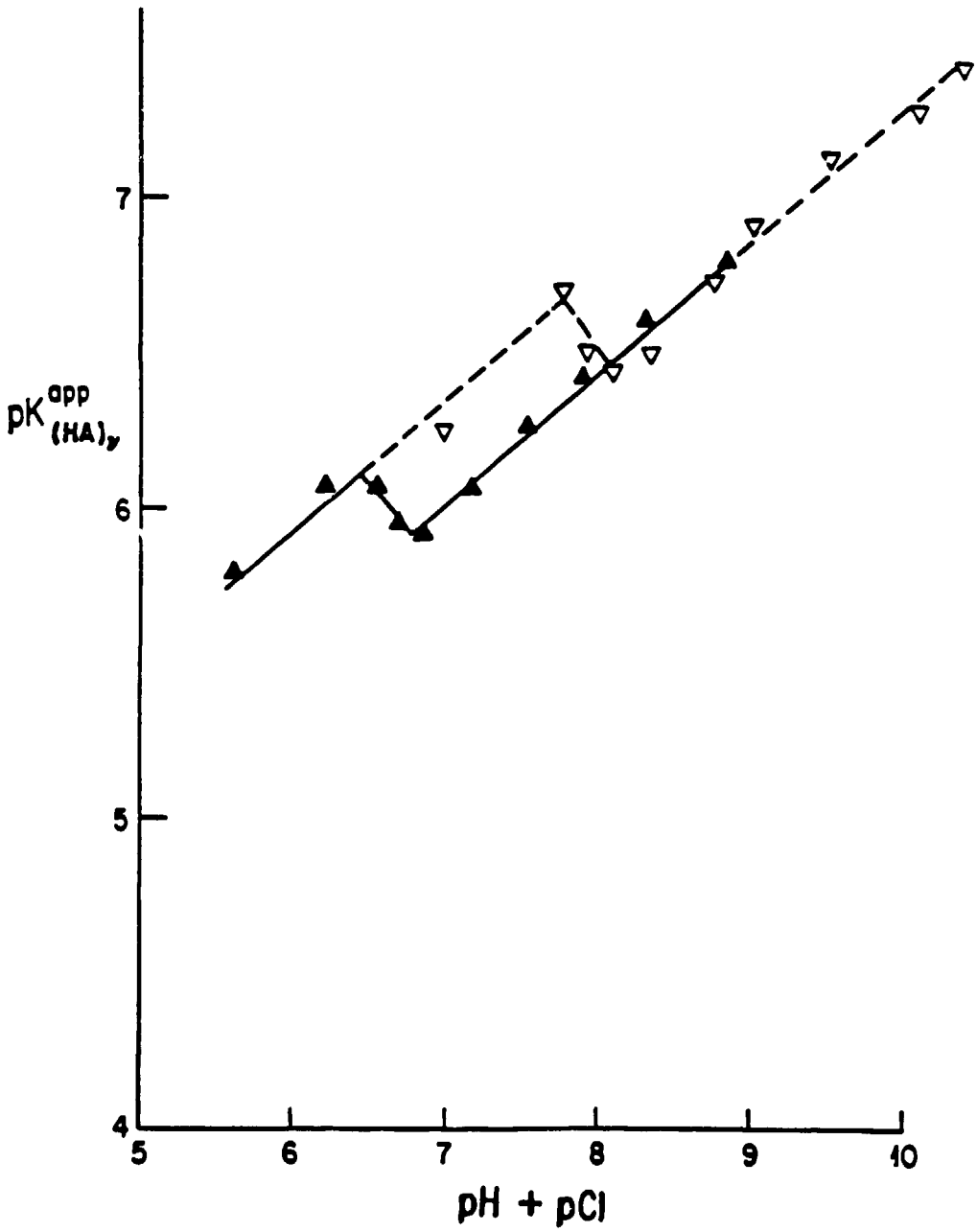

Figure 7. Apparent pK values obtained for isostatic poly (methacrylic acid) in 0.10 and 0.010 N NaCl plotted versus (pH+pCl). ▲ △

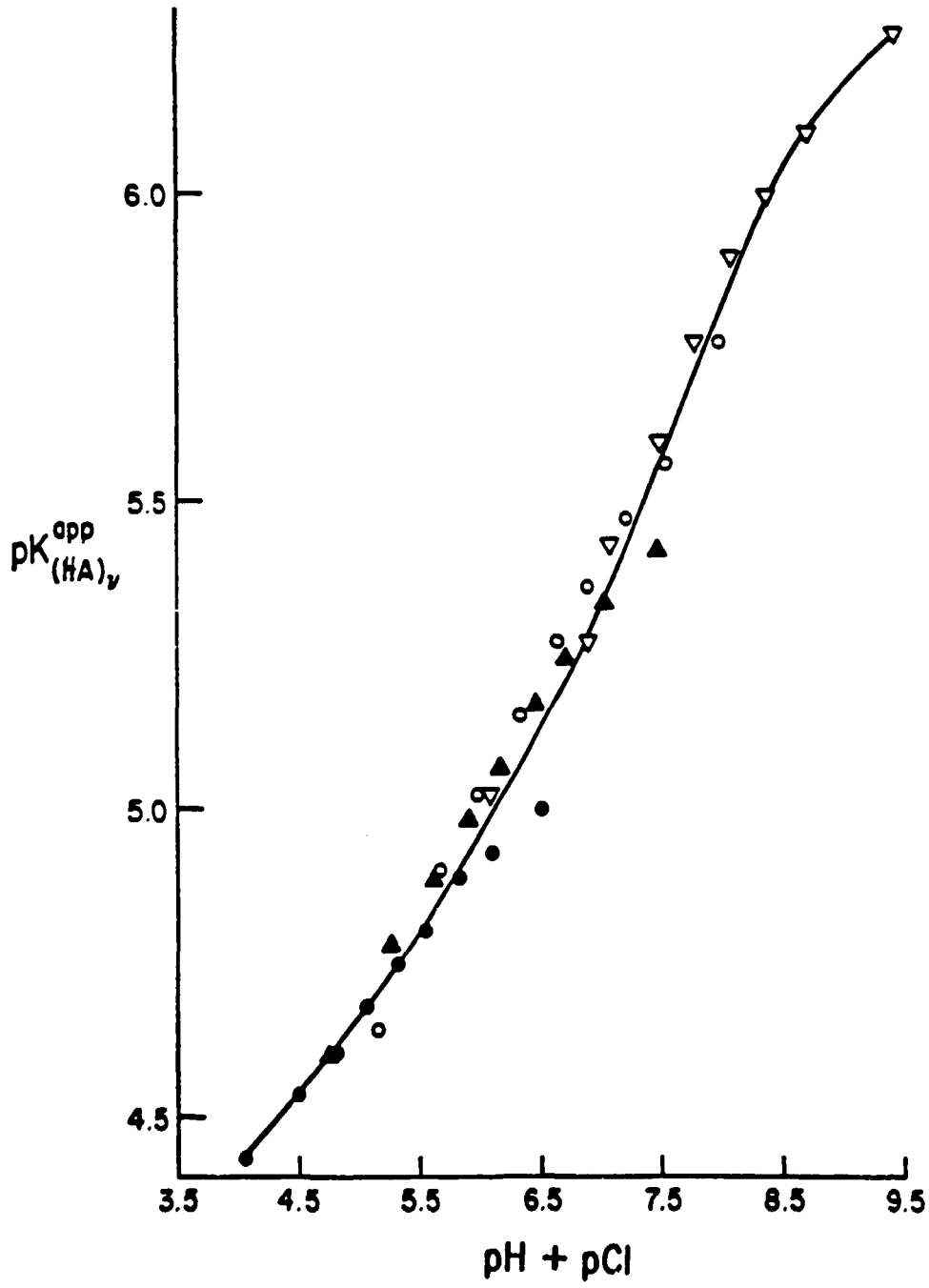

Figure 8. Apparent pK values obtained for poly (D, L-glutamic acid) at four different sodium chloride concentrations plotted versus (pH+pCl).

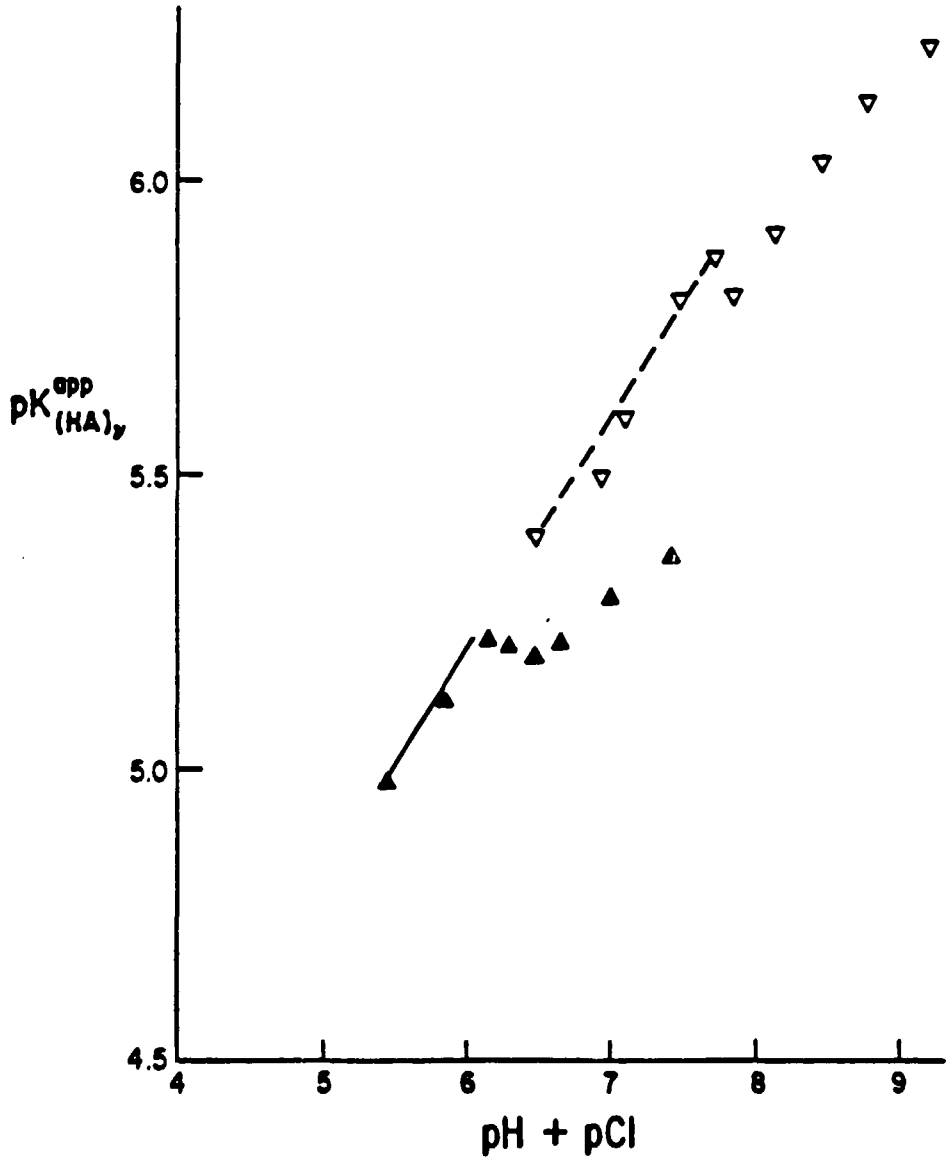

Figure 9. Apparent pK values obtained for poly (L-glutamic acid) in (▽) 0.010 and (▲) 0.10 N NaCl plotted vs. (pH+pCl).

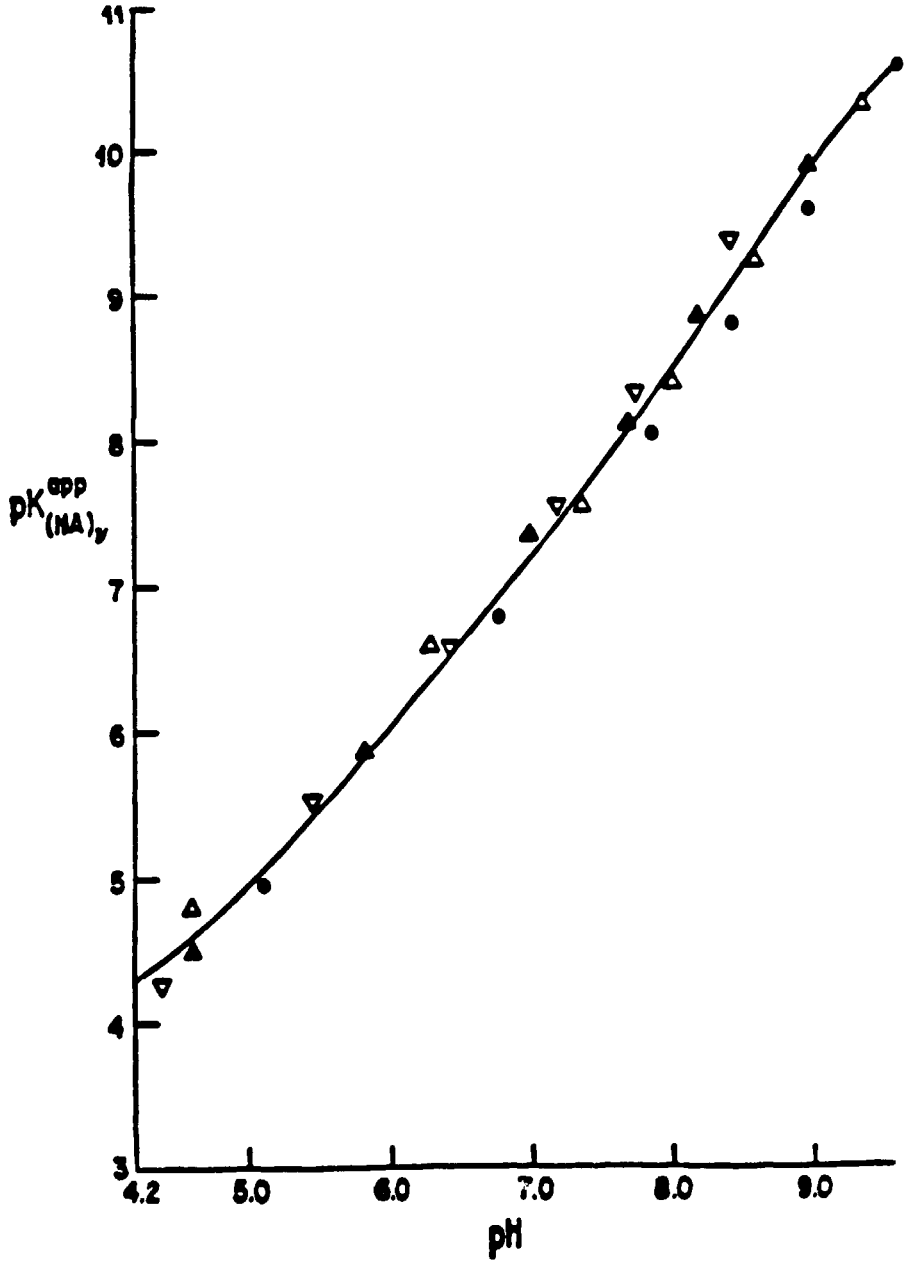

Figure 10. Apparent pK values obtained for poly(ethyleneimine) in 0.0010, 0.010, and 1.0 N NaCl plotted versus the experimental pH.

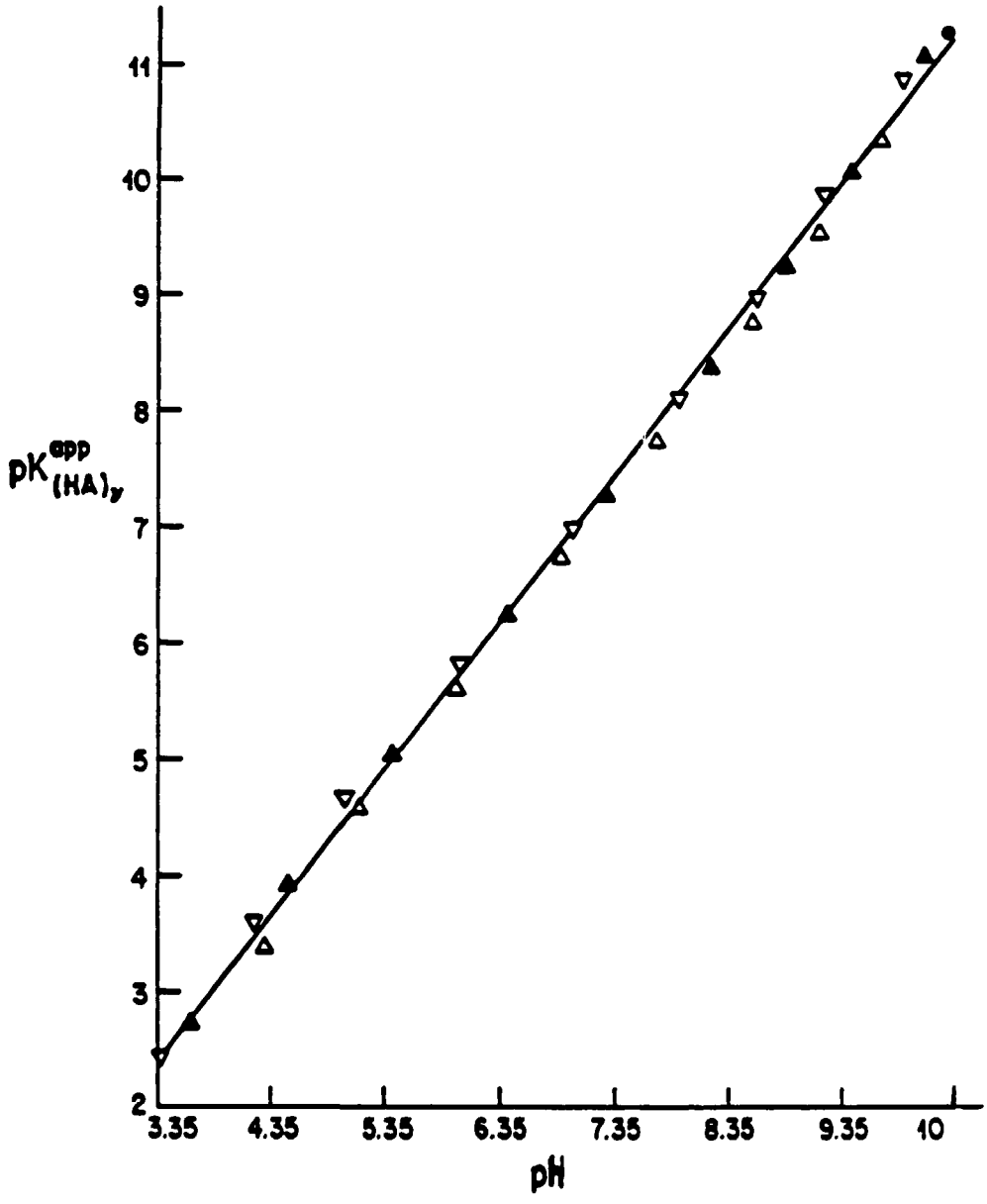

Figure 11. Apparent pK values obtained for poly (vinylamine) in 0.050, 0.10, and 1.0 N NaCl plotted versus the experimental pH.

4 APPLICABILITY OF THE TWO-PHASE MODEL TO FULVIC ACID SYSTEMS

The two-phase model describes the nature of charged polymeric molecules whether they exist as a separate gel phase or are completely dissolved in the aqueous medium employed. Their rigidity or lack of rigidity and their permeability or impermeability to simple salt can be deduced from plots of apparent pK versus (pH+pX) and pH alone. In addition, the displacement of plots of $pK^{app}_{(HA)_\nu}$ versus α as a function of ionic strength can be used to provide a basis for correction of the electrostatic disturbance of the apparent pK /24, 35-37/.

Humic and fulvic acid protonation equilibria thus, should be susceptible to analysis by the above approach if the two-phase model is applicable; the potentiometric properties of several different fulvic acid sources have been exhaustively studied by Marinsky and coworkers to examine this possibility. Pertinent data that were obtained in these studies with the Armadale Horizons Bh fulvic aid /21/ are detailed below to demonstrate the applicability of the two-phase model.

Representative potentiometric data for the Armadale Horizons Bh fulvic acid that were obtained during its titration with standard base at different concentration levels of the background electrolyte are presented in Figures 12 and 13. The data points obtained at each ionic strength with a particular fulvic acid concentration level are differentiated by the identifying symbols noted in each figure. The potentiometric curves, are insensitive to fulvic acid concentration levels from 55 ppm to 1835 ppm, and tend to converge as α approaches zero. This insensitivity to fulvic acid concentration levels is lost at 20 ppm, the potentiometric curves of a particular ionic strength value being displaced upward 0.15 to 0.2 pK units (Figure 14). This effect of lowering the fulvic acid concentration to the 20 ppm level on the potentiometric properties of the fulvic acid has not yet been explained but may be an indication of molecule elongation through head to tail interaction.

The separation of the potentiometric curves as α increases is a function of ionic strength, with divergence among the curves greatest at the lowest ionic strength employed. This behaviour suggests that the fulvic acid moiety exists in solution as a separate phase. The potentiometric curves show much less dependence on ionic strength than a typical high-molecular weight polyelectrolyte, such as poly(methacrylic acid). This result is consistent

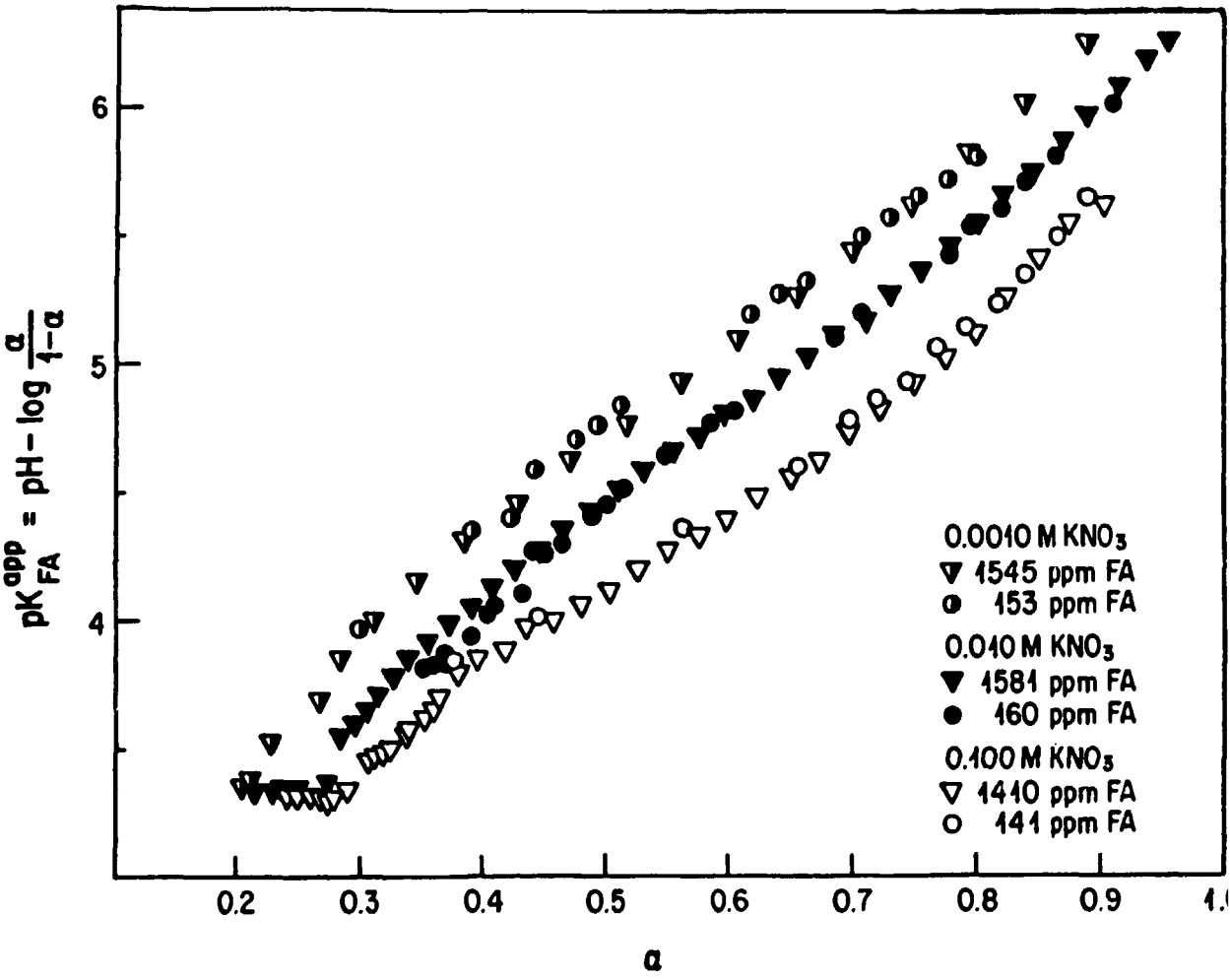

Figure 12. Variation of pK_{FA}^{app} in Armadale Horizons Bh fulvic acid with degree of dissociation at three different ionic strength levels: Ionic medium, KNO_3.

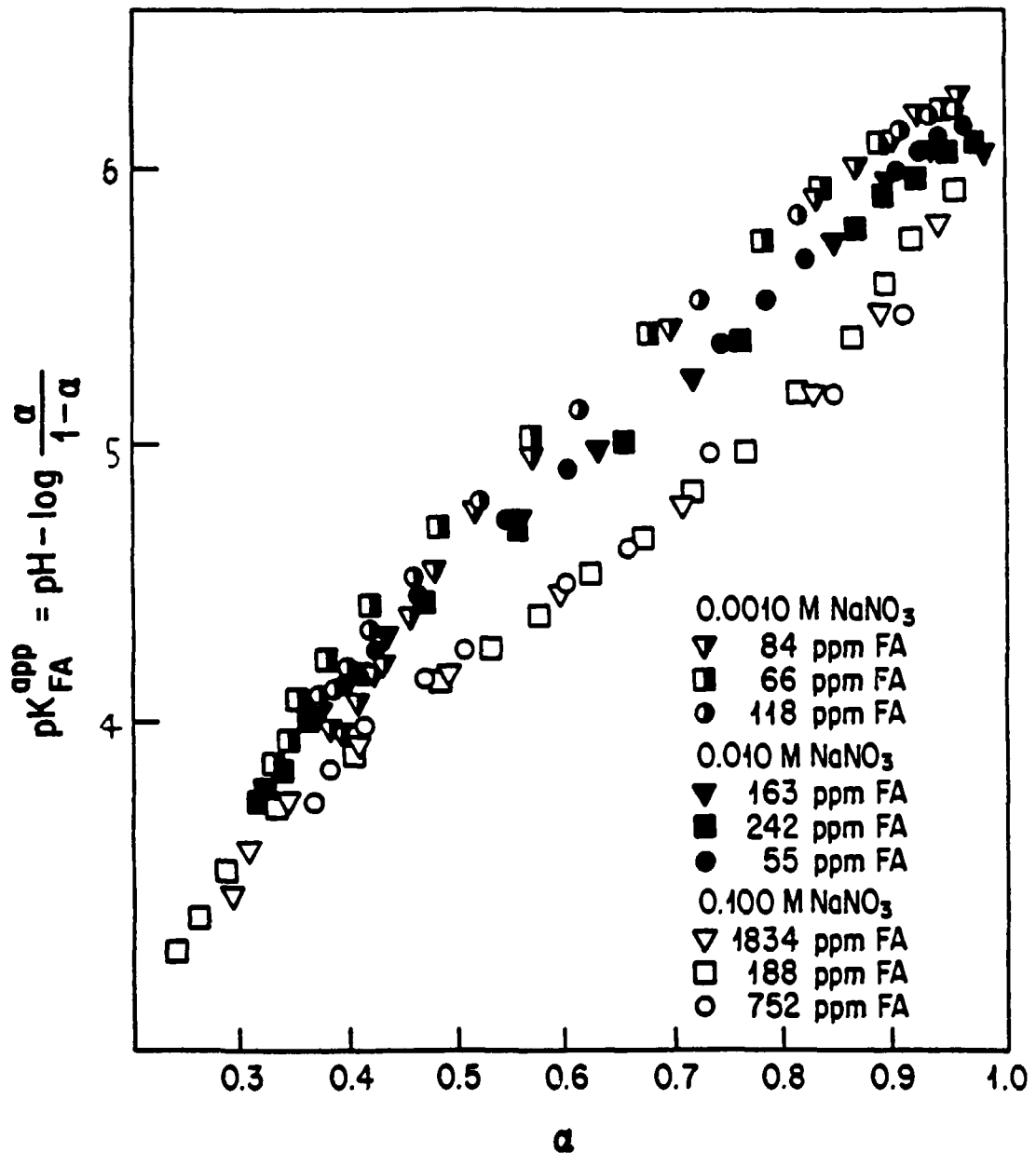

Figure 13. Variation of pK_{FA}^{app} in Armadale Horizons Bh fulvic acid with degree of dissociation at three different ionic strength levels: Ionic medium, $NaNO_3$.

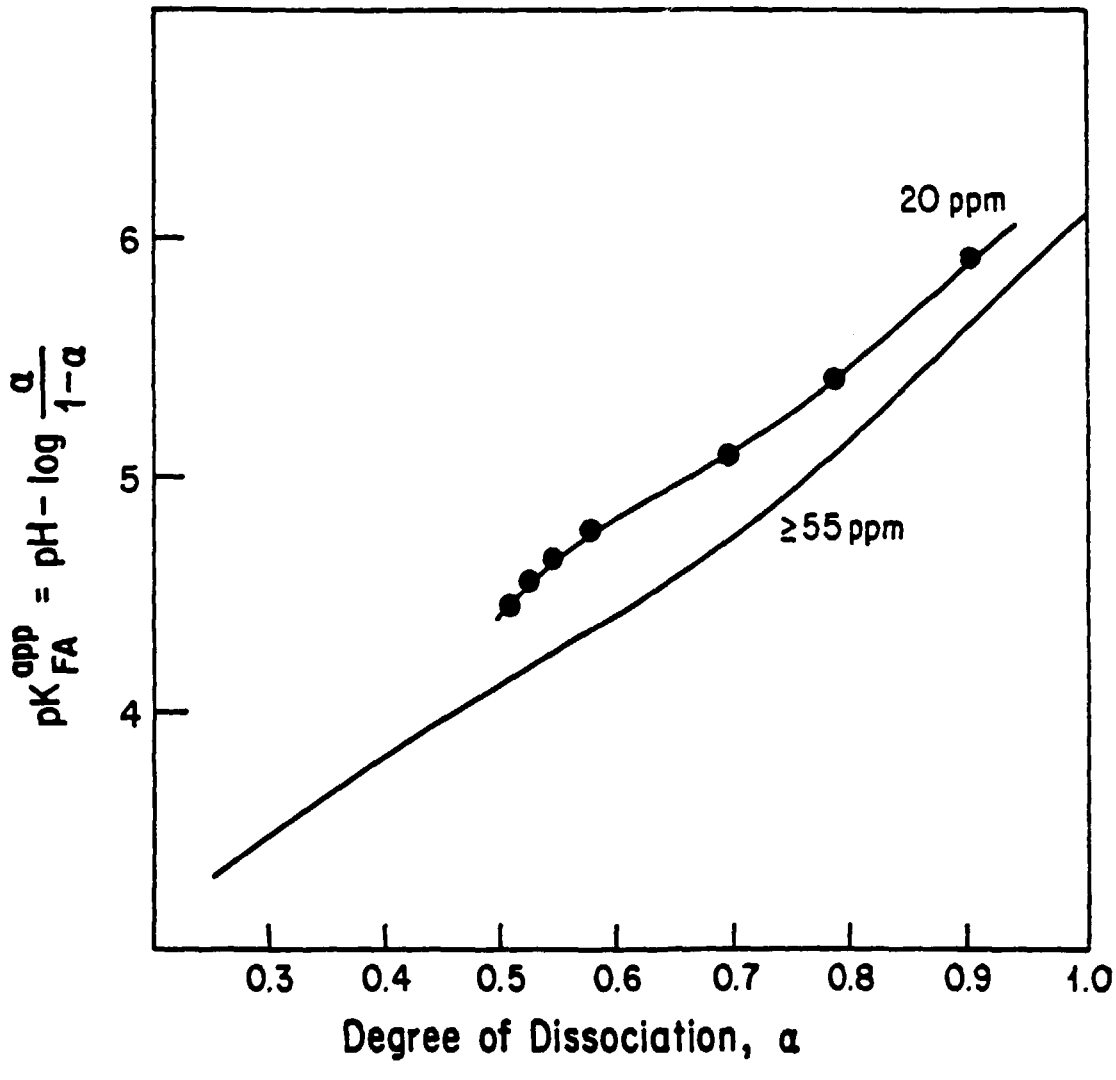

Figure 14. Effect on the pK_{FA}^{app} function of lowering FA concentration levels to 20 ppm at a fixed ionic strength (I=0.10M): Armadale Horizons Bh fulvic acid.

with end effects introduced as a result of the relatively small size of the fulvic acid moiety (MW ≈ 710) and is discussed later. The curves in Figure 15, separated from each other by the pX term, merge into a single curve when the apparent pK is plotted versus pH (Figure 16). This result, applicable to all the potentiometric data [lowest (20 ppm) to highest (1835 ppm) fulvic acid concentration levels], suggests that this fulvic acid exists as an essentially rigid, salt-impermeable polymeric moiety.

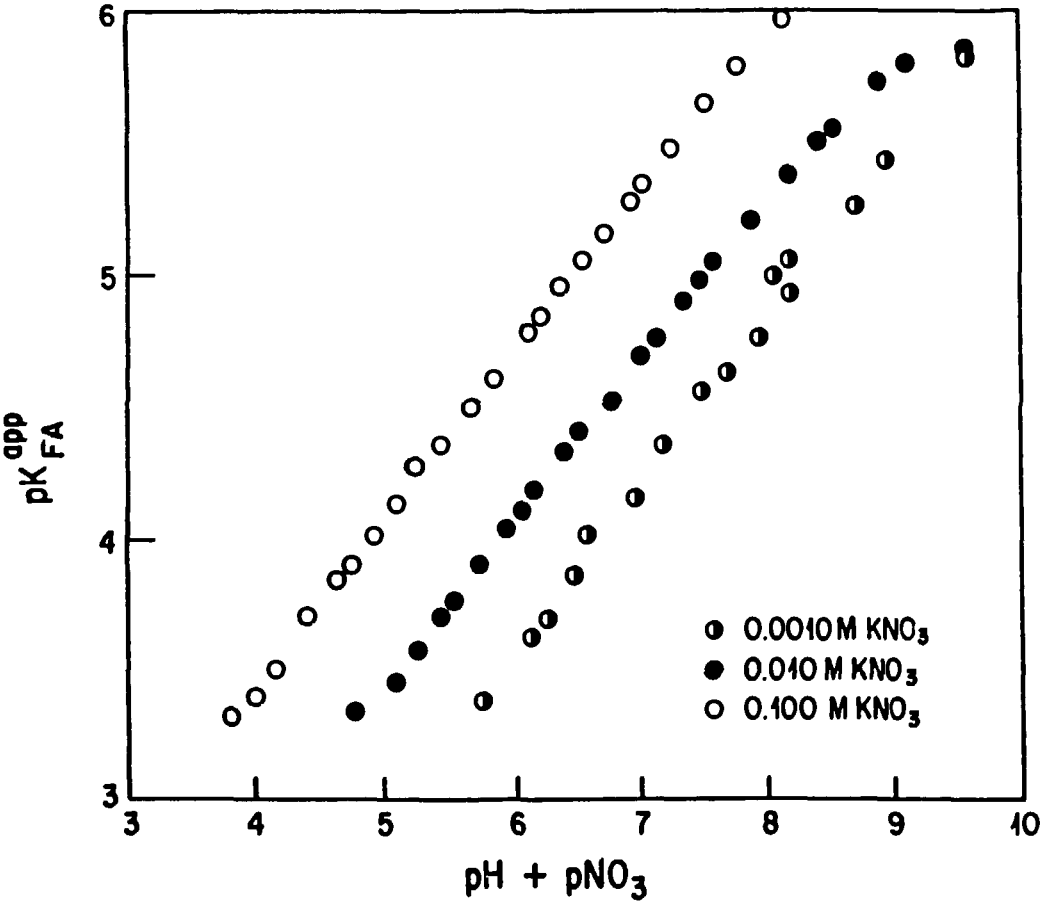

Figure 15. Variation of pH_{FA}^{app} with the ($pH+pNO_3$) term in Armadale Horizon Bh fulvic acid: Ionic strength range from 0.0010 to 0.10.

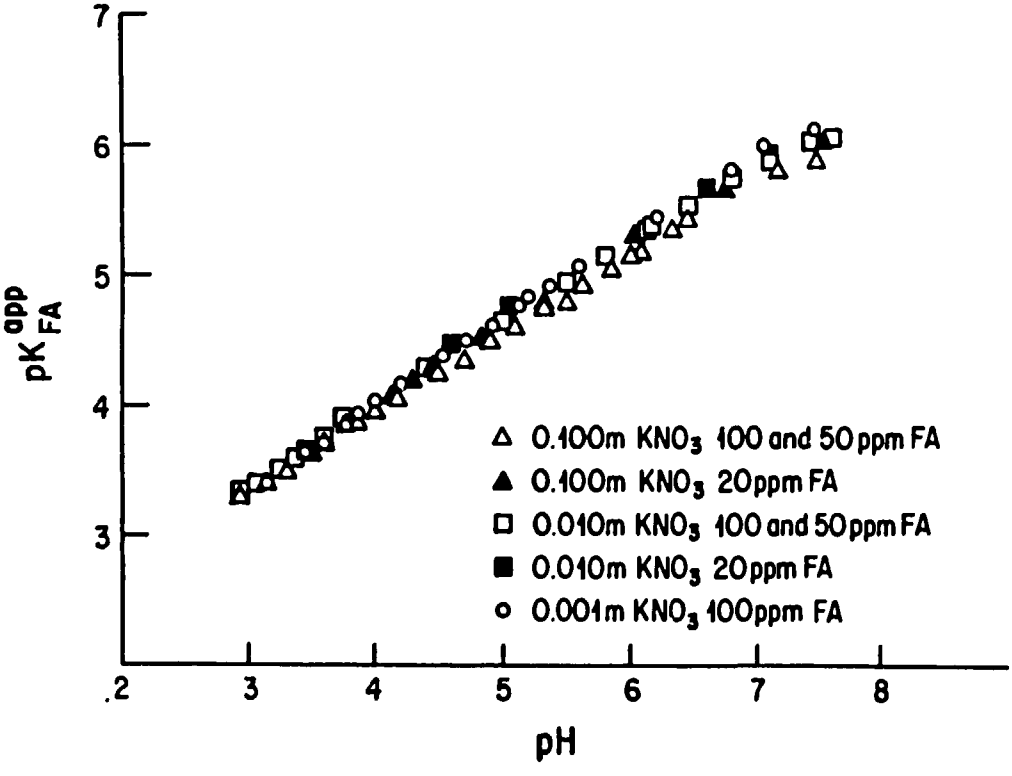

Figure 16. Variation of pK_{FA}^{app} with pH in Armadale Horizons Bh fulvic acid: Ionic strength range from 0.0010 to 0.10.

5 MODEL FOR THE INTERPRETATION OF THE PROTONATION EQUILIBRIA OF FULVIC ACID IN AQUEOUS MEDIA

5.1 CONTRIBUTION OF POLYELECTROLYTE PROPERTIES TO PROTONATION EQUILIBRIA OF FULVIC ACID IN AQUEOUS MEDIUM

The observation that the Armadale Horizons Bh fulvic acid moiety may be considered as rigid and impermeable to salt suggests that the ratio of metal ion to hydrogen ion at the molecule surface is uniquely defined by the degree of fulvic acid ionization. This ratio is mimicked in the aqueous solution as well. As long as the activity of the metal ion in the solution is lower than its activity at the molecular surface the apparent pK will be affected by ionic strength.

Increasing the salt concentration in a fulvic acid solution must, as was pointed out earlier, eventually reduce the discrepancy between surface and solution activities of M^+ to zero thereby removing the dependence of apparent pK on ionic strength.

The reduction of the extent of ionization toward zero must have this effect, as well, on the sensitivity of apparent pK to ionic strength. As α approaches zero the polymer domain charge must eventually be lowered sufficiently, even at the lowest ionic strength levels, to reach a point where the activity of M^+ inside the molecule and in the solution proper is the same. Below this point apparent pK has to be insensitive to ionic strength once again.

To test these predictions, potentiometric data were obtained at higher salt concentration levels than those presented in Figures 12 and 13 /2/. These data, obtained at I=1.0 and 5.0 M with the Armadale Horizon Bh fulvic acid are plotted in Figure 17 together with the earlier pK_{FA}^{app} versus α plots compiled at lower I values. Both of the model-based predictions are found to prevail. First, the curves obtained at the two highest salt concentration levels are nearly identical. This demonstrates no significant difference between the activity ratio of the M^+ ion in the domain of the fully dissociated fulvic acid molecule and in the solution proper (the factor proposed by the model to be responsible for the sensitivity of apparent pK to ionic strength) at a salt concentration level of 1.0 M. Second, the curves merge as the degree of ionization is lowered.

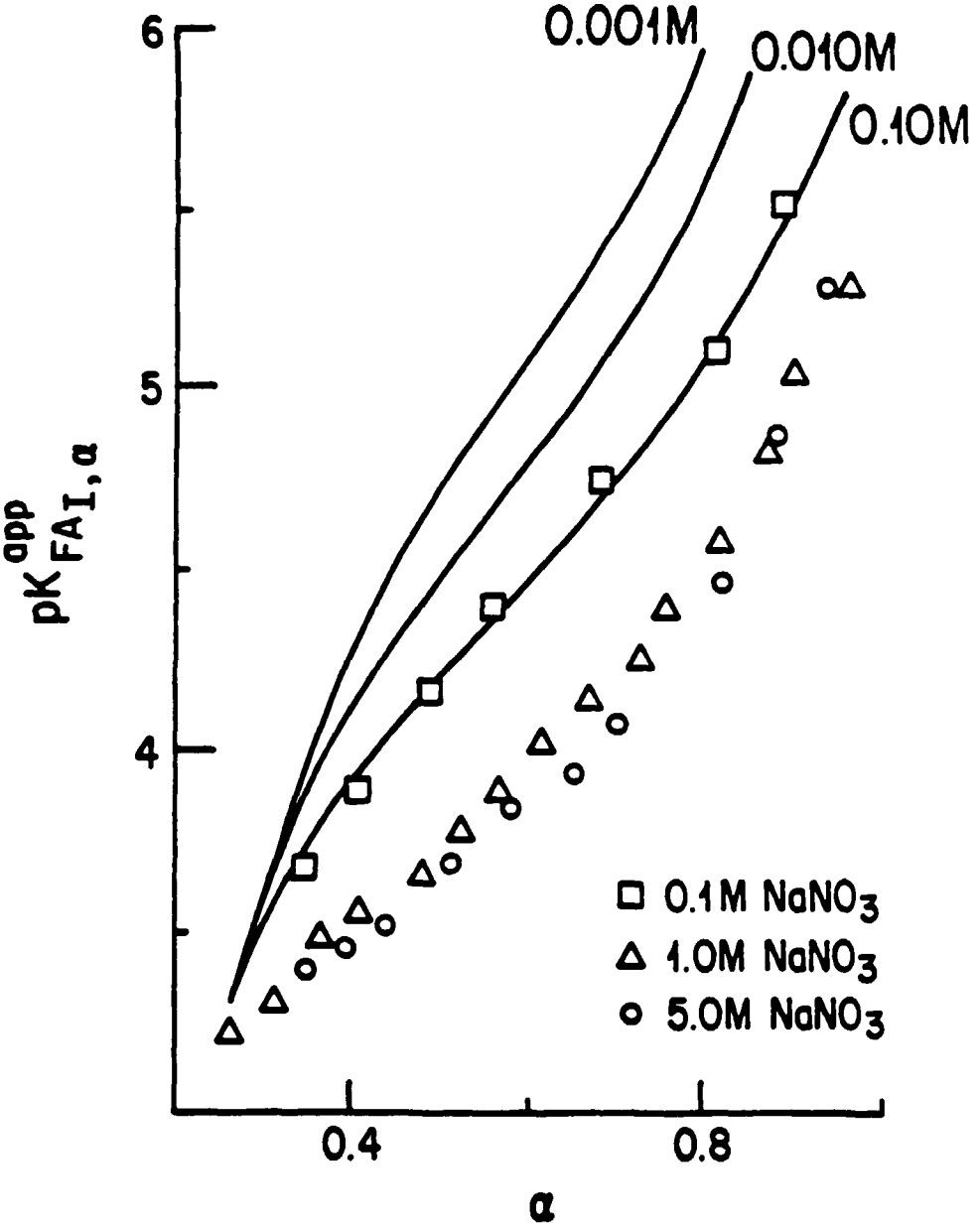

Figure 17. Insensitive of pK^{app}_{FA} to ionic strength at high neutral salt concentration levels: Armadale Horizons Bh fulvic acid.

The model, however, also predicts that a 10-fold change in the ionic strength of the excess salt medium ongoing from I=1.0 to 0.10, from I=0.1 to 0.01, and from I=0.010 to 0.0010 should have produced parallel curves displaced by one pK unit in Figure 17 as long as the activity of the M^+ ion in the polymer phase remains at least 10 times greater than the critical value of about unity reached at I=1.0 M. Instead the curves are separated eventually by 0.55, 0.45, and 0.2, respectively.

The discrepancy observed between experiment and theory, as we stated earlier, can be attributed to the fact that the fulvic acid molecule is small. Because of this, end effects become important in the cylindrically shaped molecule, the functional sites nearest the two ends of the molecule tending to behave like normal monomeric molecules. One can, on this basis, envisage the extent of departure from predicted behavior to depend on the relative contribution of the fulvic acid moiety extremities and the cylindrical portion of its rigid, impermeable, domain to the potentiometric properties.

This rationalization of the influence of end effects in the proposed model explains the small but increasing negative displacement of the pK_{FA}^{app} versus α curves with each 10-fold increase in the concentration of the neutral salt medium. As solution ionic strength increases a limiting value is reached (here this limiting value is approximately 1.0 m) beyond which pK_{FA}^{app} is no longer a sensitive function of the background salt concentration level. The activity in solution, of the metal ion at this ionic strength is identified with this limiting activity, $\vec{a}$, in the polymer domain of the fully dissociated Armadale Horizons Bh fulvic acid molecule. On this basis the polymer domain activity of the metal ion at any α value is presumed to be $\vec{a}\alpha$, neglecting the change in activity coefficient with surface concentration during the neutralization process.

With this revised model the variation of K_{FA}^{app}, the apparent dissociation constant of the fulvic acid molecule, with degree of ionization and solution ionic strength, I, when the ionic strength is less than one molar is directly related to the fractional contribution of end (x) and charged (1-x) cylinder effects in the molecule as shown in eq. 6.

$$K_{FA}^{app} = K_{FA_{lim}}^{app} [x + (1-x)\ (a/\vec{a}\alpha)] \qquad (6)$$

$$= K_{FA_{lim}}^{app} [x + 1-x\ (c/\vec{c}_{lim}\alpha)] \qquad (6a)$$

The $K_{FA_{lim}}^{app}$ parameter in this equation, obtained through interpolation of the lowest curve in Figure 17 to the desired degree of dissociation, defines the potentiometric behaviour dependence of the FA on sample heterogeneity alone. The $a/\vec{a}\alpha$ term, which relates the counterion activity ratio in the solution and polymer phases, is used as shown to reflect the effect of the surface charge of the cylindrical portion of the FA molecule on the measured value of K_{FA}^{app}. To facilitate qualitative anticipation of the effect of

this term on the measured pK_{FA}^{app} the activity ratio $a/\vec{a}\alpha$, has been presumed to be sufficiently approximated by the counterion concentration ratio, $c/\vec{c}\alpha$, in equation 6a; here $\vec{c}$ is assigned a value of unity to agree with the experimental observation that charge effects on K_{FA}^{app} are absent at this ionic strength.

Use of equation 6a is of course restricted to the experimental situation where $c/\vec{c}\alpha$ or c/α ($\vec{c} \simeq 1$) <1. One can expect this condition to be met only after an α value large enough to produce a noticeable charge effect is reached. That this is indeed the case may be seen in Figure 18 where the vertical displacement of the pK_{FA}^{app} versus α curves (I = 0.01, 0.010, and 0.0010 M) from the I=1.0 and 5.0 M curves presented in Figure 17 is plotted versus α. The curves diverge at α=0.2 to define the point at which the charge of the cylindrical domain is sufficiently developed to lead to $a/\vec{a}$ values smaller than unity. By use of values of K_{FA}^{app} and $K_{FA_{lim}}^{app}$ interpolated from Figure 18 and the c/α term developed with the model the fractional contribution of end effects to the displacement of pK_{FA}^{app} curves at the lower ionic strengths can be estimated. For the three different salt concentration levels (0.0010, 0.010, and 0.10 M) the fractional contribution of end effects is about .06, 0.09, and 0.17 respectively.

The slow increase with increasing ionic strength in the estimated fractional contribution of end effects obtained from this interpretation of the displacement of the pK_{FA}^{app} curves is believed to indicate that head-to-tail interaction between FA molecules may be promoted by a decrease in the concentration of the background electrolyte.

5.2 THE CONTRIBUTION OF FUNCTIONAL HETEROGENEITY TO PROTONATION EQUILIBRIA

An increase in the value of apparent pK, pK_{FA}^{app} with degree of ionization characterizes the potentiometric properties of the Armadale Horizons Bh fulvic acid molecule when charge effects are no longer operative (in the lowest curve presented in Figure 17). The positive slope of the $pK_{FA_{(lim)}}^{app}$ versus α curve, because of the absence of any polyelectrolyte effect, must thus have its origin exclusively in the functional group heterogeneity of the fulvic acid molecule. Site heterogeneity estimates have consequently been based on this lower curve. The final choice of functional group assignments and their abundances was based on the capability they provided for the accurate reproduction of the experimental data (2).

Functional group assignments to the fulvic acid were facilitated by potentiometric titrations conducted separately in the presence of either excess cupric or europium ion. Potentiometric titrations in nonaqueous medium and examinations of the complexation of trace-level concentrations of $^{154}Eu^{3+}$ by the fulvic acid moiety

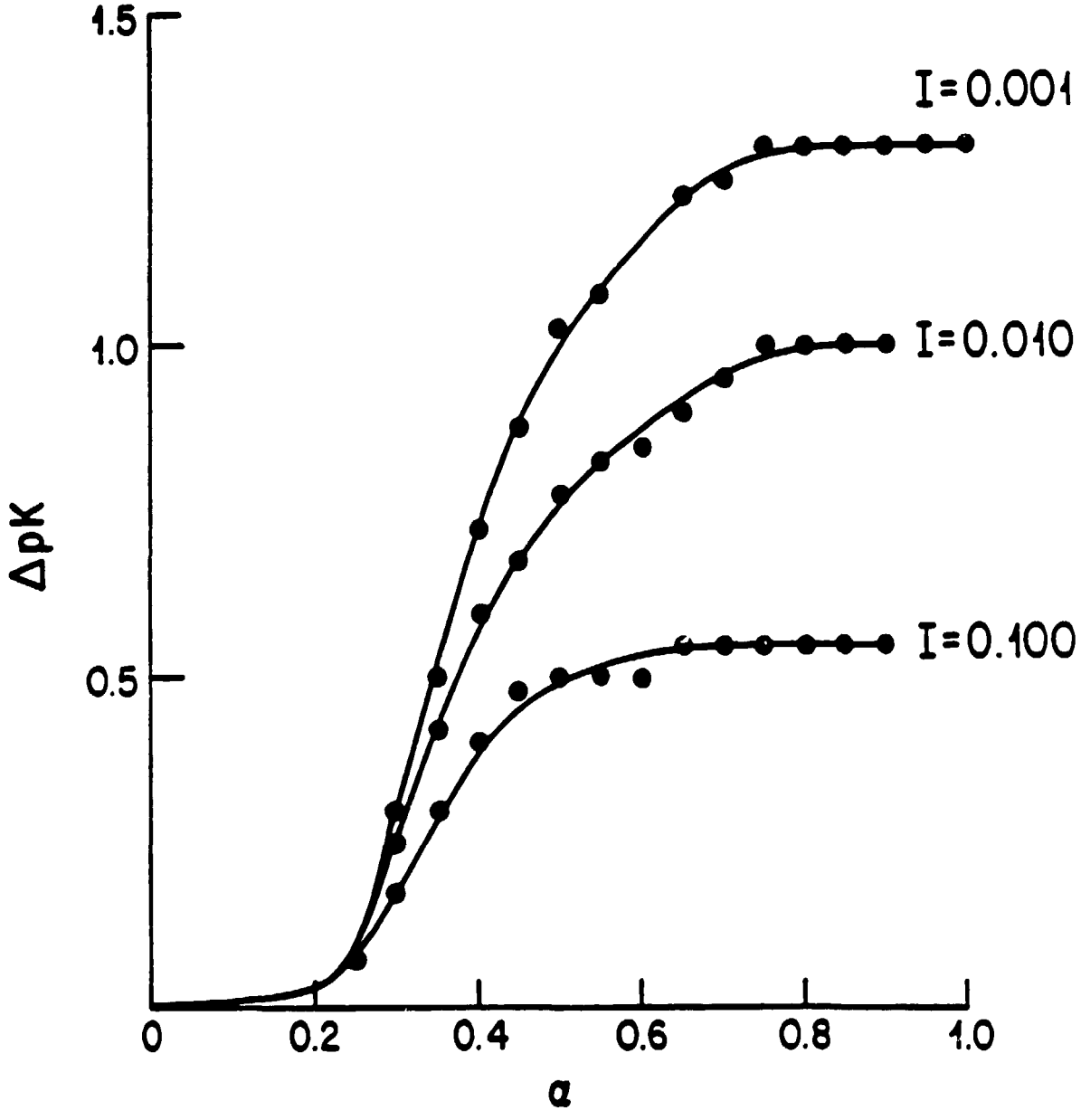

Figure 18. Variation of electrostatic deviation term (ΔpK) at three different ionic strength levels: Armadale Horizons Bh fulvic acid.

under varying conditions of pH, fulvic acid concentration, and the presence of excess simple salt /38/ provided additional information for this purpose.

From the extra release of protons observed in the chelation studies of copper ion (Figures 19 and 20) two acidic functional groups, in approximately equal quantity, and constituting about 50% of the total acidity measurable in the standard titration of fulvic acid with base, were considered to be associated with weakly acidic phenolic groups in an ortho position to them. The fact that cupric ion was strongly attached to the two chelate sites whereas europium ion was attached to only one, was the basis for identifying one of the sites with a salicylic acid-like group. The stability constant of the copper ion-salicylate complex is 4.6×10^{10} while the value reported for the europium ion-salicylate complex is only 2.75×10^{4} /25/ to lend credence to this estimate. The bidentate site that is strongly complexed by both cupric ion and europium ion has, on the basis of results obtained in complexation studies with trace-level concentrations of $^{65}Zn^{2+}$, $^{60}Co^{2+}$ and $^{154}Eu^{3+}$ /38/ and in the nonaqueous titration studies of these fulvic acids, been assigned to a dihydroxyl functional group. The acidic alcohol identified in the non-aqueous titrations /2/ was found to be present in quantities approximately equal to the extra proton released from fulvic acid by excess Eu^{+3} to suggest this proposed complexation path (Figure 21 and Table I).

Table I. Functional Group Analysis of Armadale Horizons Bh Fulvic Acid (FA) Using ρ-Hydroxybenzoic Acid (PHBA) as an Internal Reference.

		equiv points, mL of TBAH[a]		capacity, mequiv/g		
PHBA, g	FA, g	1st	2nd	COOH	OH	total
0.0920	0.0	12.55	25.10	7.20	7.20	
0.0767	0.0	10.50	21.10	7.23	7.23	
0.0829	0.0	11.50	23.00	7.30	7.30	
0.02400	0.01919	4.82	8.75	4.20[b]	1.76[b]	5.96
0.02413	0.01930	4.82	8.80	4.13[b]	1.84[b]	5.97
0.01756	0.01404	3.50	6.42	4.11[b]	1.93[b]	6.04
				4.15	1.84	5.99

[a]Molarity of TBAH = 0.0528 M. [b]After subtraction of PHBA contribution.

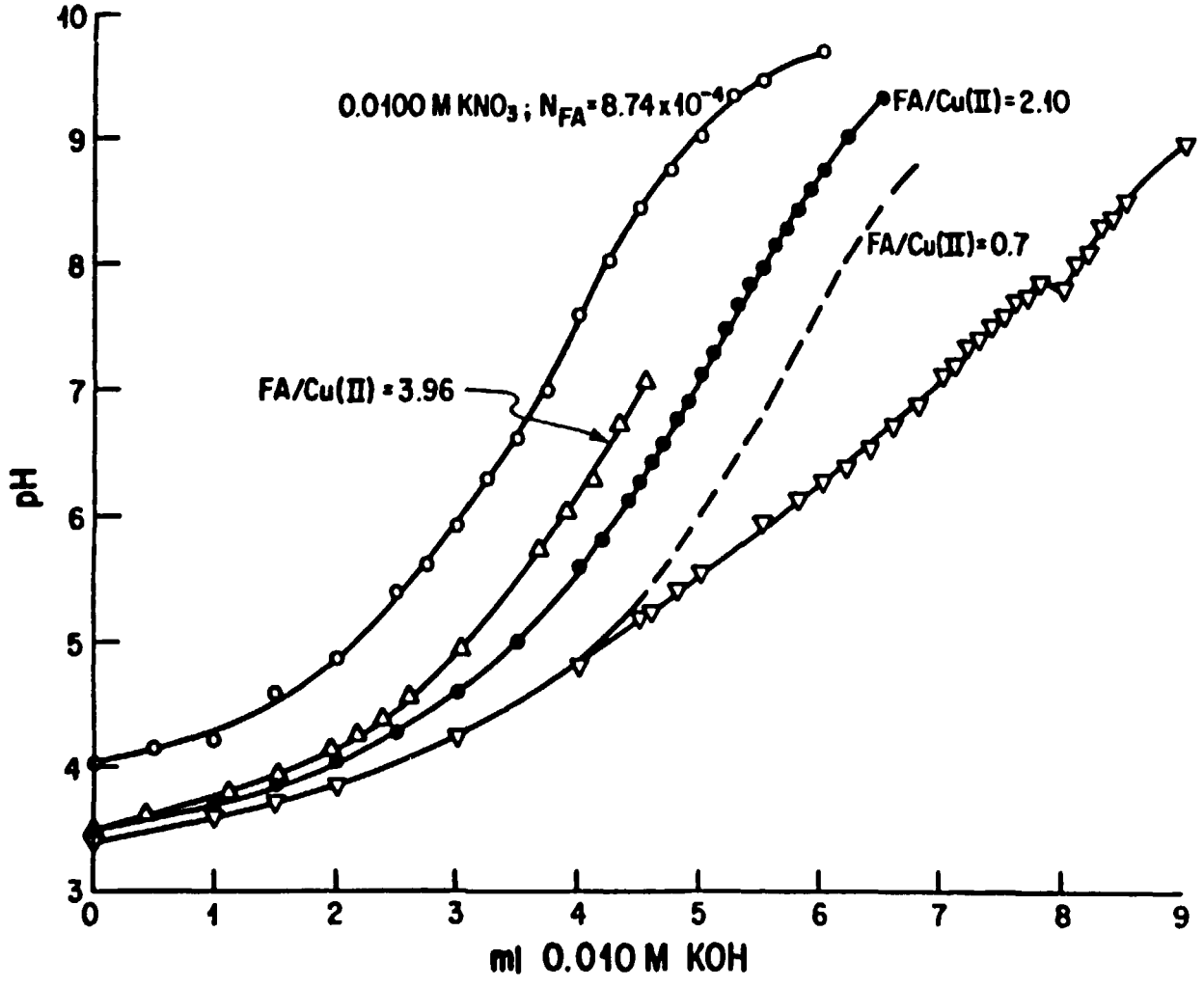

Figure 19. Proton release from Armadale Horizons Bh fulvic acid in the presence of Cu(II).

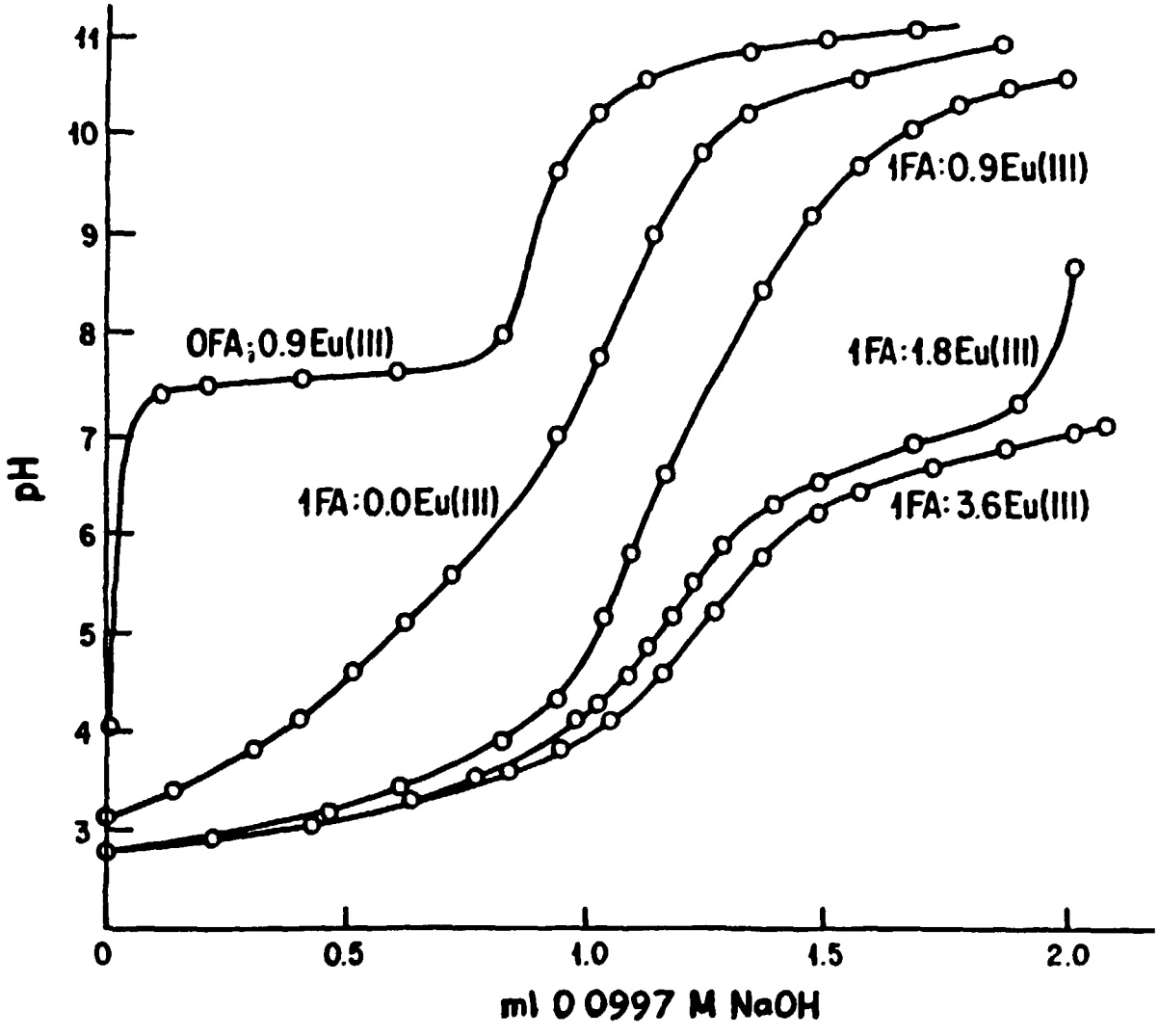

Figure 20. Proton release from weakly acidic OH groups of Armadale Horizons Bh fulvic acid in the presence of Eu (III).

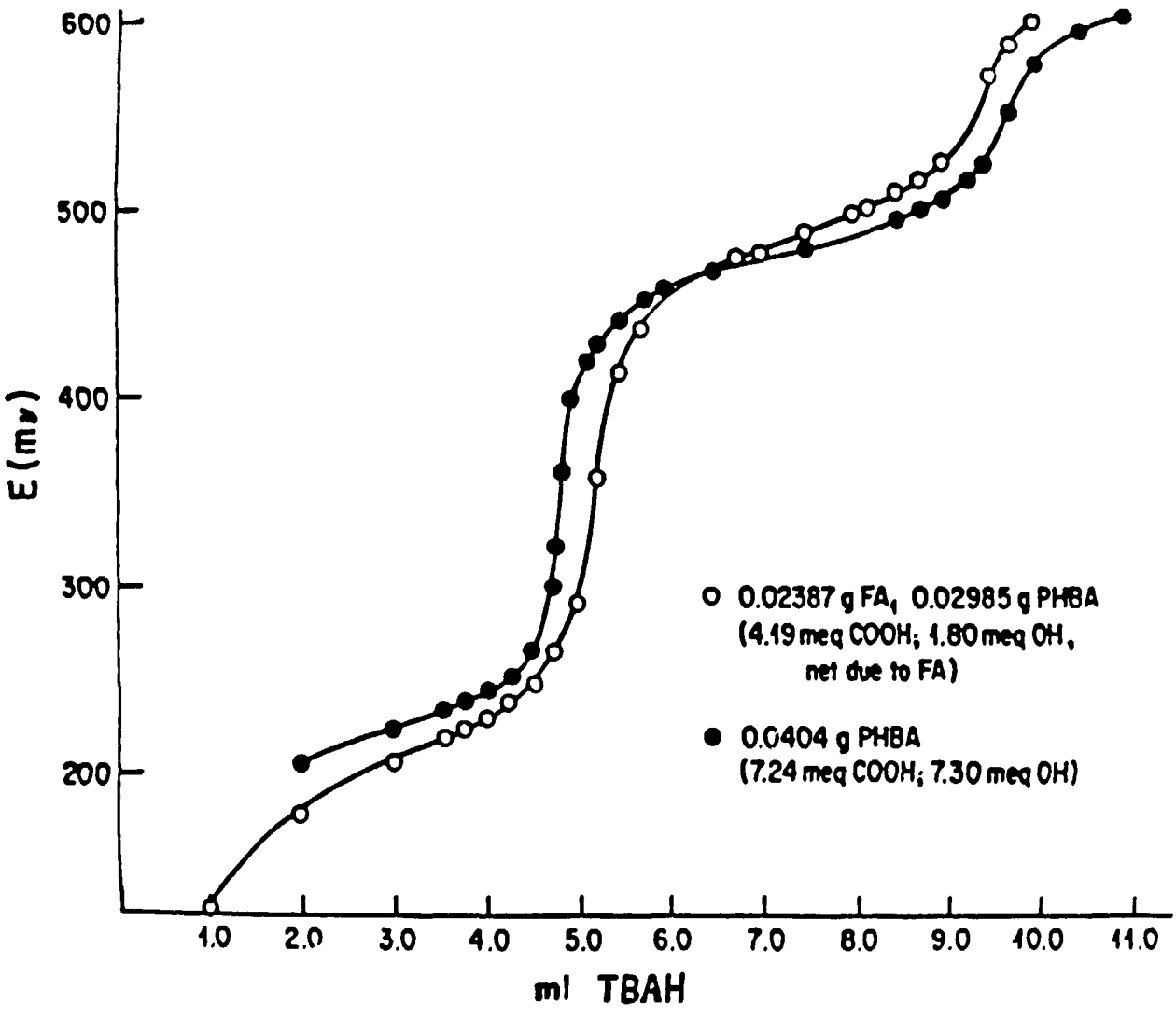

Figure 21. Potentiometric titration in DMF of THBA in the absence and presence of Armadale Horizons Bh fulvic acid.

The pK of 3.0 associated with the salicylic acid molecule and an abundance assignment of 25% were used in the first estimates to resolve the functional group heterogeneity of the Armadale Horizons Bh fulvic acid molecule. The second acidic group, with an abundance also equal to approximately 25%, was, on the basis of the trace $^{154}Eu^{3+}$ complexation studies /38/ assignable to a weakly acidic group characterized by an intrinsic pK of approximately 5.7. This weakest measurable acidic group was identified with the OH group shown by the nonaqueous potentiometric studies to constitute about 25% of the normally titratable acidity. The remaining 45-50% of the acidity had to be divided approximately equally between two more acidic groups, one relatively strong (pK ~ 1.8) and the other relatively weak (pK ≈ 4.3) to provide a $pK^{app}_{FA(lim)}$ versus α curve that mimicked the shape of the lowest titration curve presented in Figure 17.

The optimum pK and abundance, A, assignments eventually resolved were: $pK_I = 1.8$, $A_I = 0.245$; $pK_{II} = 3.2$, $A_{II} = 0.304$; $pK_{III} = 4.2$, $A_{III} = 0.24$; and $pK_{IV} = 5.7$, $A_{IV} = 0.227$. The good agreement between computed and experimentally measured species distributions by use of these parameters can be seen from careful inspection of Table II. In this table we have shown that the overall degree of dissociation measured for Armadale Horizons Bh fulvic acid at each experimental pH during its neutralization with standard base can be reproduced by computations based upon the above assignments. The sum of $A_I\alpha_I$, $A_{II}\alpha_{II}$, $A_{III}\alpha_{III}$, and $A_{IV}\alpha_{IV}$ computed at each fixed pH over the neutralization range examined in Figure 12 is in agreement with the overall experimental α values as shown in Table II to justify the proposed treatment of the fulvic acid protonation equilibria.

Table II. Comparison of Experimentally-Based Overall Degree of Dissociation, α_o^e of Armadale Fulvic Acid with Summation of Computed Contributions of Four Separate Acidic Sites to Overall Degree of Dissociation, α_o^c.

Acid Site 1, $pK_I^{int} = 1.8$; Acid Site 2, $pK_{II}^{int} = 3.4$; Acid Site 3, $pK_{III}^{int} = 4.2$; Acid Site IV, $pK_{IV}^{int} = 5.7$: Abundance, A, of Sites; $A_I = 0.245$, $A_{II} = 0.304$, $A_{III} = 0.224$, $A_{IV} = 0.227$: $\alpha_I A_I + \alpha_{II} A_{II} + \alpha_{III} A_{III} + \alpha_{IV} A_{IV} = \alpha_o^c$

pH	α_I	α_{II}	α_{III}	α_{IV}	α^c	α_o^c
2.982	0.938	0.276	0.057	0.002	0.300	0.327
3.181	0.960	0.377	0.087	0.003	0.350	0.370
3.349	0.973	0.471	0.124	0.004	0.400	0.410
3.513	0.981	0.565	0.171	0.006	0.450	0.452
3.700	0.992	0.765	0.340	0.016	0.550	0.555
4.126	0.995	0.842	0.458	0.026	0.600	0.608
4.344	0.997	0.898	0.582	0.042	0.650	0.657
4.568	0.998	0.936	0.700	0.069	0.700	0.702
4.827	0.999	0.964	0.809	0.118	0.750	0.746
5.127	1.000	0.982	0.894	0.211	0.800	0.791
5.478	1.000	0.992	0.950	0.375	0.850	0.844
5.904	1.000	0.997	0.981	0.615	0.900	0.907
6.504	1.000	0.999	0.995	0.864	0.950	0.968

6 A PROGRAM FOR ANTICIPATING METAL ION BINDING TO HUMIC AND FULVIC ACIDS IN NATURAL WATERS

6.1 COURSE OF DEVELOPMENT

Use of the fundamental aspects which control the interaction between fulvic acid and hydrogen ion as described has made it possible to reach our primary goal, the development of a program for anticipating metal ion binding to organics in natural waters /39/ in much the same way as metal ion binding to inorganics, also in natural water, is predicted /40/. The path to this capability was accomplished in the following way: With the acidic components of fulvic acid assigned to four separate moieties characterized as described in Table II the following assessment was made: Two of the four acidic units were considered, on the basis of proton release in the presence of Cu^{+2} and Eu^{+3}, to be associated in a bifunctional mode with phenolic groups too weakly acidic to be otherwise detectable in titrations with standard base. Because one of these two bidentate assemblies was, on the basis of its ability to complex Cu^{+2} much more strongly than Eu^{+3}, compared to salicylic acid with a pK_{ROOH} of 3 /25/ it was assigned to site II with a carboxylic acid moiety of comparable acidity (pK_{II}=3.2). As was mentioned earlier the Eu^{+3} tracer studies identified the weakly acidic alcohol with site IV (pK_{IV}=5.7).

To test the applicability of the complexation paths permitted by this site model for estimate of metal ion binding patterns the interaction of several metal ions to Armadale Horizons Bh fulvic acid was exhaustively examined as a function of ionic strength, metal ion to fulvic acid ratio, and degree of neutralization /2/. Predictions of the observed binding patterns were then sought by assigning literature-based stability constants /25/ to the complexes presumed to be formed by these sites. For example, the simple stability constant of 20 used for the unidentate complexes presumed to be formed with calcium ion was based on the values reported for calcium ion-carboxylate complexes in the literature. With the Ca^{+2} ion the formation constant of the unidentate complex is, because of the absence of covalency in the bond, independent of the carboxylic acid strength.

6.2 THE REFINED APPROACH

The eventual refinement of the approach developed for examining the binding of metal ions to Armadale Horizons Bh fulvic acid is outlined below: In the stepwise procedure described the interaction of Ca^{+2} ion is examined to provide an example of its application.

The information compiled in Table II is used in the first step of the procedure to resolve from the experimental pH the overall degree of dissociation of the fulvic acid as well as the fractional dissociation of the three carboxylic acid groups and the one enol group. In this first step the experimental pH is used to obtain an estimate of the apparent pK of the FA, Ca^{+2}, neutral salt system under investigation from the plot of pH versus apparent pK compiled earlier for the metal-free but otherwise similar system (Figure 16). With this assessment of apparent pK a first estimate of the fulvic acid degree of dissociation becomes accessible from the appropriate plot of apparent pK versus α obtained previously for the metal-free FA at the salt-concentration level of the experimental system (Figure 13). The plots of exp $(-\varepsilon\psi(a)/kt)$ versus α at different salt concentration levels described earlier (Figure 18) is then used to obtain the exponential value needed to reduce the experimental pH value to the pH attributable to the heterogeneity factor. The degree of dissociation determined to be associated with this reduced pH value from interpolation of the values listed in Table II should agree with the α value deduced earlier. When there is some discrepancy the above procedure needs to be repeated until modification of the apparent pK used earlier results in convergence of the two α values. The exponential value so obtained provides the appropriate correction for concentration enhancement of the free mobile counterions in the cylindrical domain of the charged molecule.

With the parameters, exp $(-\varepsilon\psi_{(a)}/kt)$, α_I, α_{II}, α_{III}, and α_{IV} made available in this manner and with reasonable estimates of the magnitude of stability parameters accessible from the literature the following sequence of computations are entered to compute the quantity of each species formed at a particular experimental pH and pCa.

To evaluate the quantity of unidentate species being formed in the course of an experiment at the carboxylic acid sites, (I, II and III) and the acidic alcohol site (IV) the same formation constant is, as mentioned earlier, presumed to characterize their respective equilibria. *Covalency is not a contributing factor* to the binding of Ca^{+2} to oxygen containing ligands and the literature value of 2.0×10^1 reported for Ca acetate$^+$ /25/ is used as shown in equation 8:

$$\beta_{CaR(COO_n)^+} = 2.0 \times 10^1 = \frac{CaR(COO_n)^+}{(Ca^{+2}_f)\ (\exp -2\varepsilon\psi_{(a)}/kt)(\gamma_{Ca^{+2}})\ (\alpha_n)\ [A_n\ (FA)_T - CaR(COO_n)^+]}$$

where the subscript n refers to either site I or site III; no second oxygen containing group is considered sufficiently close to the carboxylate moiety to provide a chelating potential; the subscript T is used in this equation (and the others that follow) to show that the total quantity of FA employed in the experiment is involved in the computation. There is correction for Debyean long-range interaction of the Ca^{+2} ion with co-ions included in the equation to reduce the measured concentration to an effective concentration. This term, denoted by $\bar{\gamma}_{Ca^{+2}}$ is available from Kielland's table of single ion activity coefficients /34/. The exp $(-\varepsilon\psi_{(a)}/kT)$ term extracted from Figure 18, is squared in equation 8 to correct for enhancement of the divalent Ca^{2+} at the site of reaction by the net electric field emanating from the charged fulvic acid molecule.

With sites II and IV, chelation reactions are competitive with the unidentate reactions and have to be taken into account. For example to evaluate the removal of Ca^{2+} from solution as both the salicylate-like chelate, $Ca(COO_{II})R(CO)$, and the competing unidentate species, $Ca(COO_{II})RCOH^{+}$, the following set of simultaneous equations needs to be solved.

$$K_{Ca(COO_{II})R(CO)} = \frac{Ca(COO_{II})RCO(a_{H^+})}{Ca_f^{2+}(\exp(-\varepsilon\psi_{(a)}/KT))(\gamma_{Ca^{2+}})(\alpha_{II})[A_{II}(FA_T)-Ca(COO_{II})R(CO)-Ca(COO_{II})RCOH^{+}]} \quad (9)$$

$$\beta_{Ca(COO_{II})COH^{+}} = \frac{Ca(COO_{II})RCOH^{+}}{Ca_f^{2+}(\exp(-2\varepsilon\psi_{(a)}/KT))(\gamma_{Ca^{2+}})(\alpha_{II})[A_{II}(FA_T)-Ca(COO_{II}R(CO)-Ca(COO_{II})RCOH^{+}]} \quad (10)$$

Equation (9) has been employed because the concentration of $(COO_{II})R(CO)^{2-}$ that is needed to describe the formation of the chelate species directly is not easily accessible. Instead we have considered the following equilibrium, which is more amenable to analysis:

$$Ca^{2+} \; (HOC)R(COO_{II}^{-}) \rightleftarrows Ca(COO_{II})R(CO) + H^{+} \quad (11)$$

Because the K for this reaction, multiplied by the formation constant of the phenolic group, is equal to $\beta_{Ca(COOII)R(CO)}$ we have assigned $K_{Ca(COOII)RCO}$ a value of 10^{-8}. The pK of the phenolic group in salicylic acid is approximately 13, and this K assignment corresponds to a β value of approximately 10^5. This β value is sufficiently smaller than the literature value /25/ of 3.6×10^5 reported for the Cd chelate (Ca is not reported) at I = 0.1 M to justify its use.

The same straightforward approach to the competitive binding of uni- and bi-dentate complexes with the OH site (site IV) is found to be unsuitable.

Preliminary binding experiments showed that site IV was more accessible to multivalent ions than could be reasonably accounted for by the formation of a dihydroxyl chelate. Rationalization of binding experiments with trace-level concentrations of multivalent ions /38 and 41/ showed that a second chelation path, defined by the substitution of a carbonyl group for 10% of the phenolic OH groups ortho to the acidic alcohol site (IV), could account for the extra binding.

This observation was effected by employing the radioactive tracer binding data in equation 12 shown below. In this equation α_S and C_S correspond, respectively, to the degree of dissociation of the unidentified complexation site and its concentration; their relationship to each other in x sets of experiments was determined through solution of (x-1) simultaneous equations arrived at by equating the left-hand side of equation 12 which is invariant

$$\frac{M_{b(exp)} - M_{b(calc)}}{(M_f^{2+})\ (\exp -z\varepsilon\psi_{(a)}/kt)(\gamma_M z+)(\alpha_S\ C_S)} = \beta_{MA}(z-1)+ \qquad (12)$$

The value of M_b (calc) used in equation 12 was obtained by estimating the quantities of unidentate and bidentate species expected to be formed using the methods described above. Their sum was subtracted from $M_{b(exp)}$, the total quantity experimentally observed to be bound. In the computation of the quantity of M^{z+} bound by the acidic alcohol as the unidentate and bidentate complexes, $MO_{IV}CRCOH^{(z-1)+}$ and $MO_{IV}CRCO^{(z-2)+}$, equations paralleling those used to anticipate such competitive binding with the salicylic acid-like group (equations 9 and 10) were used.

Such use of equation 12 eliminated the need for real values of C_S and $\beta_{MA}(z-1)+$, which cancel in the operations. The exponential term was available from Figure 18 in the following way. First the experimental pH was used in Figure 16 to extract the value of $pK^{app}_{(FA)_\nu}$ by interpolation. Figure 13 was then used to extract the value of α for the particular system. This α value was then used to find the appropriate exponential term extractable from Figure 18. The value of $\gamma_M z+$ was accessible from Kielland's computation of single ion activity coefficients /34/.

With the relative magnitude of α_x made available in this way the Henderson-Hasselbalch equation, modified as shown in equation 13, could be used to identify the site involved in the extra binding of the trace multivalent metal ion.

$$pH - \log \frac{\alpha_x}{1 - \alpha_x} - \exp\ (\varepsilon\psi_{(a)}/kT) = pK^{int}_{HS} \qquad (13)$$

To do this, it was only necessary to test the assignment of one value to α_x for use in the evaluation of the additional (x-1) values to be employed in equation 13. The eventual correct assign-

ment of an initial α_x value, if our assessment of the problem were correct, had to lead to a sequence of (α_x-1) values that resolved a constant value of pK_{HS}^{int} with equation 13. The constant value of 5.65±0.02 that was eventually resolved through the most appropriate assignment of α_x showed (1) that our assessment of the situation was correct and (2) that S had to be identified with the OH functional group assigned in the earlier protonation studies to site IV.

The extra binding in the trace-metal ion studies, when examined in equation 12 yields $\beta_{MS}(z-1)+$ values in agreement with the formation constant values published for the acetylacetonate complexes of these respective metal ions /25/ when C_S is taken to correspond to 10% of the site IV abundance in the fulvic acid molecule. This removal of 10% of the protons from the dihydroxyl site assembly is small enough to keep such revision of earlier estimates of the abundance of the dihydroxyl assembly acceptable. These earlier estimates, based on the extra proton release deduced from examination of the dihydroxyl chelation reaction with excess macro concentrations of Eu^{+3} were subject to error of this order of magnitude.

Evaluation of the simultaneous binding of Ca^{2+} to the acidic alcohol (IV) in the unidentate complex and the two bidentate chelates formed with the carbonyl and the phenol unit, respectively, used equations 14 to 16 in a manner parallelling the approach used in equations 9 and 10. In equations 14 to 16 the subscripts, u and c, are used to identify the unidentate and chelate species.

$$K_{Ca(CO_{IV}CRCO)_c} = \frac{Ca(CO_{IV}CRCO)_c \cdot a_{H+}}{Ca_f^{2+}\cdot\exp(-\varepsilon\psi_{(a)}/KT)\cdot\gamma_{Ca^{2+}}\cdot\alpha_{IV}[A_{IV}\cdot 0.9\cdot FA_T - Ca(CO_{IV}CRCO)_c - Ca(O_{IV}CRCOH)_u^+]} \quad (14)$$

$$\beta_{Ca(O_{IV}CRCHO)_u^+} = \frac{Ca(O_{IV}CRCHO)_u^+}{Ca_f^{2+}\cdot\exp(-2\varepsilon\psi_{(a)}/KT)\cdot\gamma_{Ca^{2+}}\cdot\alpha_{IV}[A_{IV}\cdot 0.9\cdot FA_T - Ca(CO_{IV}CRCO)_c - Ca(O_{IV}CRCOH)_u^+]} \quad (15)$$

$$\beta_{Ca(O_{IV}CRCO)_c^+} = \frac{Ca(O_{IV}CRCO)_c^+}{Ca_f^{2+}\cdot\exp(-2\varepsilon\psi_{(a)}/KT)\cdot\gamma_{Ca^{2+}}\cdot\alpha_{IV}[A_{IV}\cdot 0.1\cdot FA_T - Ca(O_{IV}CRCO)_c^+]} \quad (16)$$

An equation directly expressing the formation constant of the dihydroxyl-based chelate could not be used once again because of inaccessibility of the concentration of the bidentate ligand site to computation. To circumvent this difficulty as before, a K value of 2.5×10^{-6} is employed in equation 14. The product of this K value and the β value of $\sim5\times10^{9}$ arbitrarily assigned to the weakly

acidic hydroxyl group associated with the site IV enolate-bound Ca^{2+} leads to a β value of ~$1.0x10^4$ for the chelate presumed to be formed. This β value is in reasonable accord with the formation constant values of oxygen-linked bidentate complexes of Ca^{2+} /25/.

In equations 14 and 15 the abundance of the dihydroxyl group is reduced by 10% to account for the substitution with 10% frequency of a CO group for the neighboring phenolic group of this bidentate site. A formation constant of $1x10^4$ was used in equation 16 to estimate the quantity of Ca^{2+} bound by this substitute chelating group. The tracer level studies mentioned earlier /38/ yielded a β value of ~10^6 for the Co^{2+} and Zn^{2+} complexes formed with the postulated hydroxyl, carbonyl moiety and provided the basis for this assignment.

So far the entry of Ca^{+2} as free ion into the polymer domain has not been considered in the procedure outlined for estimating the Ca^{+2} inventory in FA, Ca^{+2}, neutral salt systems. Even though this portion of the Ca^{+2} is not complexed its removal to satisfy the various equilibria can reduce the measurable Ca^{+2} in solution sufficiently to require consideration. Estimate of this quantity has been accomplished, by the following approach: At equilibrium,

$$p\vec{Ca} - 2p\vec{Na} = pCa - 2pNa \qquad (2b)$$

By rearranging the non logarithmic form of the above equation the following expression for $\vec{a}_{Ca}$ is obtained:

$$\vec{a}_{Ca} = (a_{Ca})\ (\vec{a}_{Na})^2/(a_{Na})^2 \qquad (2c)$$

Reduction of the activity parameters of equation 2c into their constituent terms then leads to an expression for $\vec{m}_{Ca}$

$$\vec{m}_{Ca} = \frac{(m_{Ca})\ (\gamma_{Ca})\ (\vec{m}_{Na})^2\ (\vec{\gamma}_{Na})^2}{(\vec{\gamma}_{Ca})\ (m_{Na})^2\ (\gamma_{Na})^2} \qquad (2d)$$

Concentrations of the counterions in the polymer domain are not accessible and equation 2d has been transformed once again to yield the following more useful equation:

$$\frac{\Sigma\vec{Ca}^{2+}}{V_p} = \frac{(m_{Ca})\ (\gamma_{Ca})\ (\Sigma\vec{Na}^{+})^2\ (\vec{\gamma}_{Na})^2}{(\vec{\gamma}_{Ca})\ (m_{Na})^2\ (\gamma_{Na})^2\ (V_p)^2} \text{ and}$$

$$\Sigma\vec{Ca}^{+2} = \frac{(m_{Ca})\ (\gamma_{Ca})\ (\Sigma Na^{+})^2\ (\vec{\gamma}_{Na})^2}{(\vec{\gamma}_{Ca})\ (m_{Na})^2\ (\gamma_{Na})^2\ (V_p)} \qquad (2e)$$

To eliminate V_p from equation 2e recall that

$$\frac{\Sigma\vec{Ca}^{+}}{V_p} = \frac{(m_{Na})\ (\gamma_{Na})\ (\exp - \varepsilon\psi_{(a)}/kt)}{\vec{\gamma}_{Na}} \qquad (4a)$$

acidic hydroxyl group associated with the site IV enolate-bound Ca^{2+} leads to a β value of ~1.0×10^4 for the chelate presumed to be formed. This β value is in reasonable accord with the formation constant values of oxygen-linked bidentate complexes of Ca^{2+} /25/.

In equations 14 and 15 the abundance of the dihydroxyl group is reduced by 10% to account for the substitution with 10% frequency of a CO group for the neighboring phenolic group of this bidentate site. A formation constant of 1×10^4 was used in equation 16 to estimate the quantity of Ca^{2+} bound by this substitute chelating group. The tracer level studies mentioned earlier /38/ yielded a β value of ~10^6 for the Co^{2+} and Zn^{2+} complexes formed with the postulated hydroxyl, carbonyl moiety and provided the basis for this assignment.

So far the entry of Ca^{+2} as free ion into the polymer domain has not been considered in the procedure outlined for estimating the Ca^{+2} inventory in FA, Ca^{+2}, neutral salt systems. Even though this portion of the Ca^{+2} is not complexed its removal to satisfy the various equilibria can reduce the measurable Ca^{+2} in solution sufficiently to require consideration. Estimate of this quantity has been accomplished, by the following approach: At equilibrium,

$$p\vec{C}a - 2p\vec{N}a = pCa - 2pNa \tag{2b}$$

By rearranging the non logarithmic form of the above equation the following expression for $\vec{a}_{Ca}$ is obtained:

$$\vec{a}_{Ca} = (a_{Ca})\ (\vec{a}_{Na})^2/(a_{Na})^2 \tag{2c}$$

Reduction of the activity parameters of equation 2c into their constituent terms then leads to an expression for $\vec{m}_{Ca}$

$$\vec{m}_{Ca} = \frac{(m_{Ca})\ (\gamma_{Ca})\ (\vec{m}_{Na})^2\ (\vec{\gamma}_{Na})^2}{(\vec{\gamma}_{Ca})\ (m_{Na})^2\ (\gamma_{Na})^2} \tag{2d}$$

Concentrations of the counterions in the polymer domain are not accessible and equation 2d has been transformed once again to yield the following more useful equation:

$$\frac{\Sigma\vec{C}a^{2+}}{V_p} = \frac{(m_{Ca})\ (\gamma_{Ca})\ (\Sigma\vec{N}a^{+})^2\ (\vec{\gamma}_{Na})^2}{(\vec{\gamma}_{Ca})\ (m_{Na})^2\ (\gamma_{Na})^2\ (V_p)^2} \text{ and}$$

$$\Sigma\vec{C}a^{+2} = \frac{(m_{Ca})\ (\gamma_{Ca})\ (\Sigma Na^{+})^2\ (\vec{\gamma}_{Na})^2}{(\vec{\gamma}_{Ca})\ (m_{Na})^2\ (\gamma_{Na})^2\ (V_p)} \tag{2e}$$

To eliminate V_p from equation 2e recall that

$$\frac{\Sigma\vec{C}a^{+}}{V_p} = \frac{(m_{Na})\ (\gamma_{Na})\ (\exp - \varepsilon\psi_{(a)}/kt)}{\vec{\gamma}_{Na}} \tag{4a}$$

By substituting this expression for $\Sigma\vec{Na}^{+}/V_p$ in equation 2e a relationship for $\Sigma\vec{Ca}^{+2}$ that is accessible to computation is finally obtained.

$$\Sigma\vec{Ca}^{+2} = \frac{(m_{Ca})\ (\gamma_{Ca})\ \ (\Sigma\vec{Na}^{+})\ (\vec{\gamma}_{Na})\ (\exp - \varepsilon\psi_{(a)}/kt}{(\vec{\gamma}_{Ca})\ (m_{Na})\ (\gamma_{Na})} \qquad (2f)$$

Difficulties encountered in the estimate of the parameters, $\Sigma\vec{Na}^{+}$, $\vec{\gamma}_{Na}^{+}$, and $\vec{\gamma}_{Ca}^{+2}$, provide the major obstacle to a reasonably accurate assessment of $\Sigma\vec{Ca}^{+2}$. We believe, however, that we have successfully surmounted this barrier with the following approach: For determining the $\Sigma\vec{Na}^{+}$ quantity we have resorted to a polyelectrolyte model which equates this parameter to the product of

$$\left[\alpha \cdot A_T \cdot (1-f_{Na^+})\left(\frac{m_{Na} \cdot \gamma_{Na}}{\vec{\gamma}_{Na}}\right)\right] \div \left[\left(\frac{m_{Na} \cdot \gamma_{Na}}{\vec{\gamma}_{Na}}\right) + zm_{Ca} \cdot \gamma_{Ca(exp)}/\vec{\gamma}_{Ca}\right].$$

Here f_{Na} represents the fraction of Na^{+} ion associated with the dissociated portion of the fulvic acid molecule that escapes its domain. In weakly acidic polyelectrolytes the practical osmotic coefficient, $\phi_{p_{Na}}$, has been equated to f_{Na} /42/. To estimate f_{Na} for these computations we have, in the course of its neutralization with standard NaOH, deduced the osmotic coefficient properties of fulvic acid as a function of α from a restricted set of osmotic measurements /39/. The ϕ_p (f_{Na}) values plotted versus α in Figure 22 were used in the sample computations that lead to the Ca^{+2}-ion binding predictions presented later, but require additional experimental confirmation. With $\Sigma\vec{Na}^{+}$ accessible in this way a first estimate of the polymer domain ionic strength is made in equation 18 through assignment of V_p to the polymer domain

$$\vec{I} = \tfrac{1}{2}\ \frac{(\Sigma\vec{Ca}^{+2}(2)^2 + \Sigma\vec{Na}^{+} + \alpha A_T}{V_p} \qquad (18)$$

Since we know (1) that $\vec{m}_{Na}\ \vec{\gamma}_{Na} = m_{Na}\ \gamma_{Na}\ (\exp{-\varepsilon\psi_{(a)}}/kt)$ from equation 4a and (2) that $\vec{\gamma}_{Na}$ will be no more than 10 to 20% smaller than γ_{Na} a reasonable first estimate of $\vec{m}_{Na}$ and consequently V_p

$$\left(V_p = \frac{\Sigma\vec{Na}^{+}}{\vec{m}_{Na}}\right)$$ is possible. With this first estimate of V_p equation 2e can be used to determine the order of magnitude of $\Sigma\vec{Ca}^{+2}$ for use in equation 18 to obtain a first estimate of $\vec{I}$. With this first estimate of $\vec{I}$ $\vec{\gamma}_{Na^+}$ and $\vec{\gamma}_{Ca^{+2}}$ are calculable from the respective quotients,

$$[\gamma^{\pm}_{NaCl})^2/(\gamma^{\pm}_{KCl})]\ \vec{I} \text{ and } [(\gamma^{\pm}_{CaCl_2})^3/(\gamma^{\pm}_{KCl})^2]\vec{I},$$

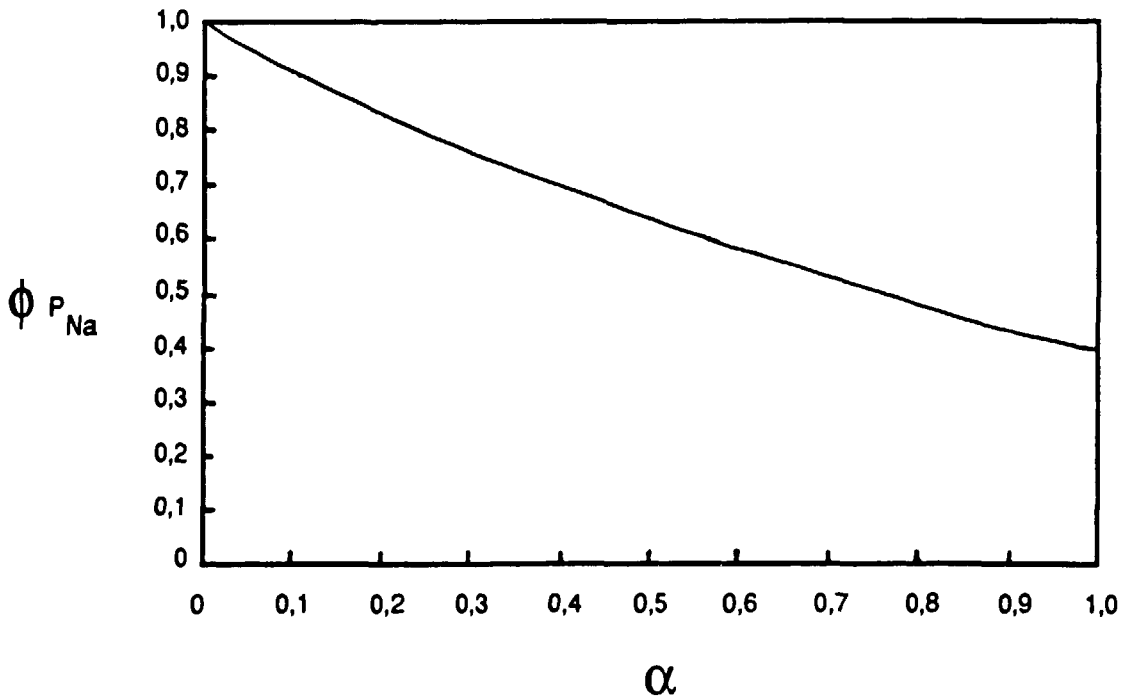

Figure 22. **Estimated osmotic properties of Armadale Horizons Bh fulvic acid as a function of α.**

obtained by using the literature-based mean molal activity coefficients of $NaCl_4$, KCl, and $CaCl_2$ at this $\vec{I}$ value /43/. With a better value of γ_{Na} now available a more accurate assessment of $\vec{m}_{Na}$ and consequently V_r, can be affected and we are ready to repeat the above sequence of operations. This second sequence of operations is usually sufficient for the successful resolution of $\Sigma\vec{C}a^{+2}$.

The quantity ($\Sigma\vec{C}a^{+2}$ + $\Sigma\vec{C}a_b$) computed in this way is compared in Table III with the total Ca^{+2} experimentally determined to be removed. There is acceptable correlation of the data by this approach in those regions of the study where small error in the measurement of free Ca^{+2} ion is not critical to the estimate of bound Ca^{+2} ion. This result lends credence to the refined model that has been developed.

Table III. The prediction of Ca^{2+}-ion binding to Armadale Horizons Bh fulvic acid as a function of ionic strength and degree of neutralization using a program that employs the measured quantities, pH and pCa.

System: 50 ml(100 ppm)AFA + 0.10 ml (0.10 M Ca(II)) titrated with 0.09982 M NaOH in 0.01 M $NaNO_3$.

ml/NaOH	pH	pCa	$\Sigma Ca_{(exp)} \times 10^3$
0.10	4.016	3.767	1.416
0.12	4.149	3.789	1.836
0.14	4.284	3.803	2.092
0.16	4.463	3.818	2.358
0.18	4.661	3.833	2.614
0.20	4.893	3.840	2.729
0.22	5.167	3.863	3.102
0.24	5.476	3.897	3.619
0.26	5.849	3.941	4.321
0.28	6.287	3.989	4.833
0.29	6.543	4.026	5.254
0.30	6.874	4.048	5.487
0.31	7.271	4.082	5.862
0.32	7.714	4.104	6.032

System: 50 ml(100 ppm)AFA + 0.10 ml (0.10 M CaII) titrated with 0.09982 M NaOH in 0.10 M $NaNO_3$

ml/NaOH	pH	pCa	$\Sigma Ca_{(exp)} x10^3$
0.24	5.350	3.762	1.292
0.26	5.740	3.772	1.487
0.27	5.980	3.783	1.698
0.28	6.245	3.793	1.886
0.29	6.564	3.810	2.196
0.30	6.940	3.817	2.313

There are, however, regions of study, where the small, unavoidable experimental error in the measurement of Ca^{+2} ion can lead to sizeable error in the estimate of bound Ca. These error sensitive regions are encountered in the early portion of the neutralization studies where the ratio of FA to Ca^{+2} is fixed. In this experimental region small error in the measurements of free Ca^{+2} ion can lead to distortion of the estimated binding results because of the small difference between the amount of Ca^{+2} added and the amount that remains detectable.

6.3 ATTAINMENT OF THE ULTIMATE GOAL; THE ADAPTATION OF THE REFINED APPROACH TO PROGRAMMING SIMILAR TO THAT USED FOR THE CONSIDERATION OF ION BINDING BY INORGANICS IN NATURAL WATERS /40/

A more practical use of the two-phase model than has so far been examined is one which would permit the accurate anticipation of free metal ion concentration in natural waters containing dissolved organic matter. The earlier procedure outlined for estimate of bound metal ion from the measured free metal ion concentration level and from the pH of the system is only satisfying from the fact that the agreement between experiment and computation has been sufficient to demonstrate the merit of the approach.

With the above demonstration of the validity of our model, however, the more practical and highly desirable goal is now accessible. We are in a position to show that two-phase approach can be used to anticipate the free metal ion content of natural waters containing organic matter. To demonstrate this let us consider a particular aqueous system containing known quantities of fulvic acid, calcium and neutral salt at a particular acidity (pH). This is the kind of information that is accessible for natural waters. With such information (pH, M_{FA}, I, m_{Ca}) the quantity, ΣCa^{+2}, can be computed as outlined in the preceding section using the quantity, $[Ca^{+2}]/gH_2O$ as our first estimate of the molality of Ca^{+2} ion, $m_{Ca^{+2}}$, in the aqueous system. The amounts of bound Ca^{2} (4 unidentate and 3 chelate species) are also susceptible to analysis by the procedures outlined earlier with use of this

initial Ca^{+2} molality parameter. The difference between $(\{\Sigma\vec{C}a^{+2} + \Sigma\vec{C}a_b\}/gH_2O)$ and $m_{Ca}{}^{+2}$, so obtained, provides a more realistic $m_{Ca}{}^{+2}$ value which is then used to reevaluate

$$(\{\Sigma\vec{C}a^{2+} + \Sigma\vec{C}a_b^{2+}\}/gH_2O)$$

These operations need to be repeated only until the $m_{Ca}{}^{+2}$ value obtained from this difference converges with the $m_{Ca}{}^{+2}$ value used in the computations.

The applicability of this approach to the anticipation of free metal ion in FA, neutral salt systems as a function of acidity (pH) and ionic strength (I), can be seen from the results of such analysis of the two Armadale FA, Ca^{+2}, NaCl systems that are summarized in Table IV which follows. In this table pH, $pCa_{(exp)}$ and $pCa_{(comp)}$ are listed for the same systems analyzed earlier in Table III. The agreement between $pCa_{(exp)}$ and $pCa_{(comp)}$ is satisfying and shows that the ultimate objective of our research has been achieved. An approach amenable to programming similar to that used in the consideration of ion binding by inorganics in natural waters is being developed /39/.

Table IV. The prediction of Ca^{2+}-ion binding to Armadale Horizons Bh Fulvic Acid as a function of ionic strength and degree of neutralization using a program that employs only the measured pH.

System: 50 ml(100 ppm)AFA + 0.10 ml (0.100 M Ca(II)) titrated with 0.09982 M NaOH in 0.010 M $NaNO_3$.

ml/NaOH	pH	$pCa_{(exp)}$	$pCa_{(calc)}$	$\Sigma Ca_{(exp)}$ x10^3	$\Sigma Ca_{(cal)}$ x10^3
0.10	4.016	3.767	3.742	1.416	0.932
0.12	4.149	3.789	3.762	1.836	1.392
0.14	4.284	3.803	3.777	2.092	1.627
0.16	4.463	3.818	3.801	2.358	2.075
0.18	4.661	3.833	3.833	2.614	2.624
0.20	4.893	3.840	3.854	2.729	2.972
0.22	5.167	3.863	3.890	3.102	3.527
0.24	5.476	3.897	3.936	3.619	4.182
0.26	5.849	3.941	3.983	4.321	4.773
0.28	6.287	3.989	4.020	4.833	5.203
0.29	6.543	4.026	4.027	5.254	5.278
0.30	6.874	4.048	4.041	5.487	5.423
0.31	7.271	4.082	4.066	5.862	5.673
0.32	7.714	4.104	4.086	6.032	5.874

System: 50 ml(100 ppm)AFA + 0.10 ml (0.10 M Ca(II)) titrated with 0.09982 M NaOH in 0.100 M $NaNO_3$

ml/NaOH	pH	$pCa_{(exp)}$	$pCa_{(calc)}$	$\Sigma Ca_{(exp)}$ x10^3	$\Sigma Ca_{(calc)}$ x10^3
0.24	5.350	3.762	3.740	1.292	0.861
0.26	5.740	3.772	3.748	1.487	1.016
0.27	5.980	3.783	3.751	1.698	1.084
0.28	6.245	3.793	3.754	1.886	1.139
0.29	6.564	3.810	3.757	2.196	1.211
0.30	6.940	3.817	3.774	2.313	1.543

REFERENCES

1 Schnitzer, M.; Kahn, S.V.; 1972, "Humic Substances in the Environment", Marcel Dekker, Inc., New York, NY.

2 Marinsky, J.A.; Ephraim, J.; Mathuthu, A.; Alegret, S.; Bicking, M.; Malcolm, R.; 1986, Environ. Sci. Technol., 20, 364.

3 Sposito, G.; Holtzclaw, K.M.; 1977, Soil Sci. Soc. Am. J., 41, 330.

4 Sposito, G.; Holtzclaw, K.M.; Kerch, D.A.; 1977, Soil. Sci. Soc. Am. J., 41, 1119.

5 Eberle, S.H.; Feurstein, W.; 1979, Naturwissenschaften, 66, 572.

6 Gamble, D.S.; 1970, Can. J. Chem., 48, 2662.

7 Gamble, D.S.; 1972, Can. J. Chem., 50, 2680.

8 Burch, R.D.; Langford, C.H.; Gamble, D.S.; 1978, Can. J. Chem., 56, 1196.

9 Shuman, M.S.; Collins, G.J.; Fitzgerald, R.J.; Olsson, D.L.; 1983, In "Aquatic and Terrestrial Humic Materials"; Christman, F.R., Gjessing, E.G.; Eds.; Ann Arbor Sci., Ann Arbor, MI, 387.

10 Perdue, E.M.; Lyttle, C.R.; 1983, Environ. Sci. Technol., 17, 654.

11 Choppin, G.R.; Kulberg, J.; 1978, J. Inorg. Nucl. Chem., 40, 651.

12 Takamatsu, T.; Yoshida, T.; 1978, J. Soil, Sci., 125, 377.

13 Plechanov, N.; Josefsson, B.; Dyrsen, D.; Lundquist, K.; 1983, In "Aquatich and Terrestrial Humic Materials", Christman, F.R.; Gjesing, E.G.; Eds.; Ann Arbor Sci., Ann Arbor, MI, 349.

14 Dempsey, B.A.; O'Medlia, C.R.; 1983, In "Aquatic and Terrestrial Humic Materials", Christman, F.R.; Gjessing, E.G.; Eds., Ann Arbor Sci., Ann Arbor, MI, 239.

15 Pommer, A.M.; Breger, I.A.; 1960, Geochim. Cosmochim. Acta, 10, 30.

16 Hruizenga, D.K.; Kester, D.R.; 1979, Linol. Oceanogr., 24, 145.

17 Varney, M.S.; Mantoura, R.F.C.; Whitfield, M.; Turner, D.R.; Riley, J.P.; 1981, In "Trace Metals in Seawater", Proceedings of the NATO Conference, 751.

18 Posner, A.M.; 1964, In "Proceedings of the 8th International Congress of Science", Bucharest, Roumania, Part II.

19 Wilson, D.E.; Kinney, P.; 1977, Limnol. Oceanogr., 22, 281.

20 Marinsky, J.A.; 1985, J. Phys. Chem., 89, 5294.

21 Marinsky, J.A., 1986, Environ. Sci. Technol., 20, 349.

22 Rossotti, J.C.F.; Rossotti, H.; 1961, "The Determination of Stability Constants", McGraw Hill Book Company, London, England, 86. Ibid, 253.

23 Helfferich, F. 1962, "Ion Exchange", McGraw Hill Book Company, New York, New York.

24 Marinsky, J.A.; Slota, P.; 1980, in "Ions in Polymers", Advances in Chemistry Series, American Chemical Society, Washington, DC; 311.

25 Myers, G.E.; Boyd, G.E.; 1956, J. Phys. Chem., 60, 521.

26 Gekko, K.; Naguchi, H.; 1975, Biopolymers, 14, 2555.

27 Sillen, L.J.; Martell, A.; 1964, "Stability Constants of Metal Ion Complexes", The Chemical Society, Burlington House, London, England.

28 Marcus, R.A.; 1957, J. Chem. Phys., 23, 1057.

29 Prigogine, I.; Mazus, P.; Defay, R.; 1953, J. Phys. Chem., 50, 146.

30 Paterson, R.; Rahman, H.; 1984, J. Colloid Interface Sci., 97, 423.

31 Nagusawa, M.; Murose, T.; Kondo, K.; 1965, J. Phys. Chem., 69, 4005.

32 Olander, D.S.; Holtzer, A.; 1968, J. Am. Chem. Soc., 90, 4549.

33 Bloy von Treslong, C.J.; Staverman, A.J.; 1974, Recl. Trav. Chim. Pays-Bas, 93, 171.

34 Kielland, J.; 1937, J. Am. Chem. Soc., 59, 1675.

35 Marinsky, J.A.; Lim, F.G.; Chung, C.; 1983, J. Phys. Chem., 87, 3139.

36 Marinsky, J.A.; Merle, Y.; 1984, Talanta, 31, 199.

37 Marinsky, J.A.; Alegret, S.; Escalos, M.T.; 1974, Talanta, 31, 683.

38 Ephraim, J.; Cramer, S.; Marinsky, J.A.; 1985, unpublished data.

39 Reddy, M.M.; Marinsky, J.A.; 1987, in preparation.

40 Lloyd, M.; Wycherley, V.; Nronk, C.B.; 1951, J. Chem. Soc., 1786. 1976 "MINEQL, A Computer Program for the Calculation of Chemical Equilibrium Composition of Aqueous Systems", Tech Note 18, Civil Eng., Massachusetts Institute of Technology, Cambridge, Massachusetts.

41 Ephraim, J.; Mathuthu, A.; Alegret, S.; Cramer, S.J.; Marinsky, J.A.; 1985, unpublished data.

42 Katchalsky, A.; Alexandrowicz, Z.; Kedem, O., 1966, in "Chemical Physics of Ionic Solutions", B.E. Conway and R.G. Barrodas, Eds., John Wiley and Sons, New York, New York.

43 Robinson, R.A.; Stokes, R.H., 1970, "Electrolyte Solutions", 2nd Edition, Butterworths, London, England.

List of SKB reports

Annual Reports

1977–78
TR 121
KBS Technical Reports 1 – 120.
Summaries. Stockholm, May 1979.

1979
TR 79–28
The KBS Annual Report 1979.
KBS Technical Reports 79-01 – 79-27.
Summaries. Stockholm, March 1980.

1980
TR 80–26
The KBS Annual Report 1980.
KBS Technical Reports 80-01 – 80-25.
Summaries. Stockholm, March 1981.

1981
TR 81–17
The KBS Annual Report 1981.
KBS Technical Reports 81-01 – 81-16.
Summaries. Stockholm, April 1982.

1982
TR 82–28
The KBS Annual Report 1982.
KBS Technical Reports 82-01 – 82-27.
Summaries. Stockholm, July 1983.

1983
TR 83–77
The KBS Annual Report 1983.
KBS Technical Reports 83-01 – 83-76
Summaries. Stockholm, June 1984.

1984
TR 85–01
Annual Research and Development Report 1984
Including Summaries of Technical Reports Issued during 1984. (Technical Reports 84-01–84-19)
Stockholm June 1985.

1985
TR 85-20
Annual Research and Development Report 1985
Including Summaries of Technical Reports Issued during 1985. (Technical Reports 85-01-85-19)
Stockholm May 1986.

1986
TR 86-31
SKB Annual Report 1986
Including Summaries of Technical Reports Issued during 1986
Stockholm, May 1987

1987
TR 87-33
SKB Annual Report 1987
Including Summaries of Technical Reports Issued during 1987
Stockholm, May 1988

Technical Reports

1988

TR 88-01
Preliminary investigations of deep ground water microbiology in Swedish granitic rocks
Karsten Pedersen
University of Göteborg
December 1987

TR 88-02
Migration of the fission products strontium, technetium, iodine, cesium and the actinides neptunium, plutonium, americium in granitic rock
Thomas Ittner[1], Börje Torstenfelt[1], Bert Allard[2]
[1]Chalmers University of Technology
[2]University of Linköping
January 1988

TR 88-03
Flow and solute transport in a single fracture. A two-dimensional statistical model
Luis Moreno[1], Yvonne Tsang[2], Chin Fu Tsang[2], Ivars Neretnieks[1]
[1]Royal Institute of Technology, Stockholm, Sweden
[2]Lawrence Berkeley Laboratory, Berkeley, CA, USA
January 1988

ISSN 0284-3757

CM Tryck AB, Bromma 1988